HEPATOLOGY
Official Journal of the American Association for the Study of Liver Diseases

Hepatitis C Virus 1b Viral Factors (Core, NS3, and NS5A) and Increased Risk of Hepatocellular Carcinoma

See Article on Page 555

Hepatitis C virus (HCV) continues to infect millions of people worldwide and remains a leading cause of serious liver diseases such as fibrosis, cirrhosis, and hepatocellular carcinoma (HCC). A majority of the patients (~70%-80%) with acute infection fail to eliminate this virus and consequently develop chronic hepatitis C (CHC).[1-3] Hepatic cancer resulting from HCV infection is a rapidly rising reason for cancer-related deaths in the United States.[4] Although there is no effective vaccine, the future of HCV antiviral therapy appears optimistic with the advent of direct-acting antiviral agents (DAAs).

HCV is an enveloped positive-strand, RNA virus belonging to the family Flaviviridae. Hepatocytes are the primary sites of replication. HCV induces rearrangement of intracellular membranes resulting in formation of membranous webs, which serve as scaffolds for the assembly of replication complexes.[5] The viral genome consists of a single open reading frame (ORF), which is flanked by 5′ and 3′ nontranslated regions. This ORF encodes for a polyprotein that is cotranslationally and posttranslationally cleaved by host and viral proteases to yield at least 10 proteins. These include three structural (core, E1, and E2) and seven nonstructural (p7, NS2, NS3, NS4A, NS4B, NS5A, and NS5B) proteins. Infectious virus particles are assembled on the surface of cytoplasmic lipid droplets (LDs).[6] Thus, the viral life cycle is a complex multistep process. It requires a large number of host cellular proteins in addition to viral. The main goal of antiviral therapy is to cure CHC by a sustained elimination of the virus, also called sustained virological response (SVR, undetectable serum HCV-RNA for 6 months posttreatment cessation).[1]

Is there a direct or indirect role for HCV in HCC? HCV has a remarkable ability to cause chronic infection, which eventually leads to HCC. In the majority of CHC patients, inflammation results in fibrosis, followed by cirrhosis. It is well known that cirrhosis increases the risk for HCC. However, in a marginal case, HCC develops even in the absence of cirrhosis, signifying that HCV is directly oncogenic.[8] Over the past few years, enormous substantiation for the ability of viral proteins to modulate important host gene functions (transcription, cell proliferation, and apoptosis) have also emerged. The expression of core protein in transgenic mice can induce HCC.[9] Another multifunctional HCV protein, NS3, has protease, helicase, and NTPase activities.[1,10] NS3 also promotes carcinogenesis[11] by interacting with p53 in an NS3 sequence-dependent manner.[12] HCV-Core protein expression both *in vitro* and *in vivo* has a direct effect on mitochondria and results in oxidative stress.[13] Oxidative stress, ROS, repeated liver damage and repair can eventually lead to HCC. Even though there have been advances, we do not understand the precise mechanism by which HCV infection results in HCC. Knowledge of this specific mechanism would allow us to intervene and prevent HCC. The frequency of HCC has tripled over the past 2 decades, while the 5-year survival rate has remained below 12% in the U.S.[4] In this issue of HEPATOLOGY, El-Shamy et al.[14] have asked an important question regarding the role of viral factors (HCV 1b) in HCC development. While it is known that viral factors impact the outcome of HCV therapy, this study further proposes the possibility of a link between HCV 1b isolates and HCC. The authors report specific sequences of the structural (Core) and nonstructural (NS3 and NS5A) proteins that associate with the development of HCC.

In this retrospective study, the authors selected 49 patients infected with HCV genotype 1b who eventually developed HCC. In addition, 100 HCV-infected

Abbreviations: CHC, chronic hepatitis C; DAA, direct-acting antiviral agent; HCV, hepatitis C virus; ISDR, interferon sensitivity-determining region; LD, lipid droplet; ORF, open reading frame; PKR, protein kinase R; SVR, sustained virological response.

Address reprint requests to: Suresh D. Sharma, Department of Biochemistry and Molecular Biology, Pennsylvania State University, 201 Althouse Laboratory, University Park, PA 16802. E-mail: sds20@psu.edu

View this article online at wileyonlinelibrary.com.
DOI 10.1002/hep.26362
Potential conflict of interest: Nothing to report.

patients who did not develop HCC, even after 15 years of follow-up, served as a control group. All patients were confirmed for CHC by liver biopsy and there was no significant difference in viral load between the two groups. The study outcome led the authors to propose that patients infected with HCV isolates with core-Gln70 and NS3-Tyr1082/Gln1112 have a higher risk to develop HCC compared to those who lacked these residues. HCV core protein is the main structural component of the viral nucleocapsid and has also been proposed to be involved in a wide array of functions such as modulating viral and cellular gene expression, host signaling pathways, and lipid metabolism.[15] Amino acid residues at position 70 and 91 in the core protein have been associated with the outcome of the standard of care (SOC) treatment, specifically in Japanese patients infected with HCV 1b. A few studies have also suggested a correlation between polymorphism at positions 70 and 91 of core protein (HCV 1b) and progression to HCC.[16,17]

The present study clearly demonstrates a greater propensity of HCV 1b isolates with core-Q70 and NS3-Y1082/Q1112 residues to cause HCC. How does the expression of core-Gln70 and NS3-Tyr1082/Gln1112 proteins contribute to HCC? Viral proteins are multifunctional, therefore perturbed interactions with signaling molecules, resulting in out-of-order signaling pathways, can be anticipated. Interestingly, a recent study found that the substitution pattern in the HCV 1b-core region does influence very early viral dynamics during the treatment (SOC plus telaprevir).[18] The amino acid residues in the NS3 protease at positions 1082 and 1112 reported in this study are near the catalytic triad (His-1083, Asp-1107, and Ser-1165) of NS3-protease.[10] It has also been shown that the N-terminal protease domain of NS3 transforms cells in culture.[8,11,12] However, the mechanism by which these polymorphic viral factors could affect virus-host interactions, as a result initiate, and finally cause HCC, needs further investigation. These studies will also help to further understand the complex life cycle of HCV. Many interesting questions can be asked: for instance, could phosphorylation of Y residues have an impact on the NS3 (protease or helicase) activity? Could these modified or unmodified residues alter protein-protein or protein-nucleic acid interactions in hepatocytes? It would be interesting to investigate these questions further.

NS5A is a proline-rich, RNA binding[19] zinc metalloprotein with three proposed structural domains (domain I, II, and III) which are separated by two low complexity sequences.[20] Owing to the high degree of conformational flexibility, domain II (DII) and domain III (DIII) are intrinsically disordered. This high degree of flexibility in D II and III imparts NS5A with the ability to interact with an array of biological partners. Domain II contains the interferon sensitivity-determining region (ISDR) which overlaps with protein kinase R (PKR) binding site. Mutations in this central region of NS5A-ISDR are reported to associate with treatment response in HCV 1b patients.[1] In the current study, Asn residue at position 2218 of the NS5a protein was detected more frequently in pre-HCC isolates than in the control isolates. It is worth noting that this Asn residue is located in the ISDR (D II) region of NS5A. The significance of this observation is not clear and more studies are required to fully understand and elucidate its role in HCC development, if any.

Another part of the study looked at the evolution of core, NS3, and NS5A-IRRDR sequences during the interval between CHC and HCC. No significant change in sequences occurred (core-Q-70, NS3-Y1082/Q1112 residues) in a progression from CHC to HCC. Interestingly, an IRRDR region in the post-HCC isolates showed a very high degree of sequence heterogeneity. NS5A-Domian III contains the IFN-RBV resistance-determining region (amino acids 2334-2379).[21] The current study found that a high degree of heterogeneity in the IRRDR region was significantly associated with HCC. This difference between pre- and post-HCC sequence in IRRDR suggests that this region evolves rapidly during the course of HCV infection, conceivably due to strong selective pressure. This region is intrinsically disordered, known to interact with multiple host factors, and, most important, also regulates virus production and consequently pathogenesis.[6]

In conclusion, the present study argues that HCV-1b isolates with core-Q-70, NS3-Y1082/Q1112 residues or NS5A-IRRDR$\geq$6 are significantly associated with HCC. These clinical studies provide the basis for a broader investigation of viral populations in a hope to decipher the precise mechanism leading to HCC. More important, such studies can also help in the design of vaccines matched to dominant/circulating viruses. Rigorous research and development efforts have led to the discovery of several DAAs. High hopes are pinned on the forthcoming DAAs, which have the potential to boost the treatment potency and eliminate the morbidity and mortality associated with CHC.

SURESH D. SHARMA, PH.D.
Department of Biochemistry and Molecular Biology, Pennsylvania State University, University Park, PA

References

1. Sharma SD. Hepatitis C virus: molecular biology & current therapeutic options. Indian J Med Res 2010;131:17-34.
2. Sklan EH, Charuworn P, Pang PS, Glenn JS. Mechanisms of HCV survival in the host. Nat Rev 2009;6:217-227.
3. Gelman MA, Glenn JS. Mixing the right hepatitis C inhibitor cocktail. Trends Mol Med 2010 [Epub ahead of print].
4. El-Serag HB. Hepatocellular carcinoma. N Engl J Med 2011;365:1118-1127.
5. Reiss S, Rebhan I, Backes P, Romero-Brey I, Erfle H, Matula P, et al. Recruitment and activation of a lipid kinase by hepatitis C virus NS5a is essential for integrity of the membranous replication compartment. Cell Host Microbe 2011;9:32-45.
6. Appel N, Zayas M, Miller S, Krijnse-Locker J, Schaller T, Friebe P, et al. Essential role of domain III of nonstructural protein 5a for hepatitis C virus infectious particle assembly. PLoS Pathog 2008;4:e1000035.
7. Nelson DR, Jensen DM, Sulkowski MS, Everson G, Fried MW, Gordon SC, et al. Hepatitis C virus: a critical appraisal of new approaches to therapy. Hepat Res Treat 2012:138302.
8. Yeh MM, Daniel HD, Torbenson M. Hepatitis C-associated hepatocellular carcinomas in non-cirrhotic livers. Mod Pathol 2010;23:276-283.
9. Ray RB, Lagging LM, Meyer K, Ray R. Hepatitis C virus core protein cooperates with ras and transforms primary rat embryo fibroblasts to tumorigenic phenotype. J Virol 1996;70:4438-4443.
10. Raney KD, Sharma SD, Moustafa IM, Cameron CE. Hepatitis C virus non-structural protein 3 (HCV NS3): a multifunctional antiviral target. J Biol Chem 2010;285:22725-22731.
11. Sakamuro D, Furukawa T, Takegami T. Hepatitis C virus nonstructural protein NS3 transforms NIH 3t3 cells. J Virol 1995;69:3893-3896.
12. Deng L, Nagano-Fujii M, Tanaka M, Nomura-Takigawa Y, Ikeda M, Kato N, et al. NS3 protein of hepatitis C virus associates with the tumour suppressor p53 and inhibits its function in an NS3 sequence-dependent manner. J Gen Virol 2006;87(Pt 6):1703-1713.
13. Okuda M, Li K, Beard MR, Showalter LA, Scholle F, Lemon SM, et al. Mitochondrial injury, oxidative stress, and antioxidant gene expression are induced by hepatitis C virus core protein. Gastroenterology 2002;122:366-375.
14. El-Shamy A, Shindo M, Shoji I, Deng L, Okuno T, Hotta H. Polymorphisms of the Core, NS3, and NS5A proteins of hepatitis C virus genotype 1b associate with development of hepatocellular carcinoma. HEPATOLOGY 2013;58:555-563.
15. Hoffman B, Liu Q. Hepatitis C viral protein translation: mechanisms and implications in developing antivirals. Liver Int 2011;31:1449-1467.
16. Akuta N, Suzuki F, Kawamura Y, Yatsuji H, Sezaki H, Suzuki Y, et al. Amino acid substitutions in the hepatitis C virus core region are the important predictor of hepatocarcinogenesis. HEPATOLOGY 2007;46:1357-1364.
17. Kobayashi M, Akuta N, Suzuki F, Hosaka T, Sezaki H, Kobayashi M, et al. Influence of amino-acid polymorphism in the core protein on progression of liver disease in patients infected with hepatitis C virus genotype 1b. J Med Virol 2010;82:41-48.
18. Akuta N, Suzuki F, Hirakawa M, Kawamura Y, Yatsuji H, Sezaki H, et al. Amino acid substitutions in the hepatitis C virus core region of genotype 1b affect very early viral dynamics during treatment with telaprevir, peginterferon, and ribavirin. J Med Virol 2010;82:575-582.
19. Huang L, Hwang J, Sharma SD, Hargittai MR, Chen Y, Arnold JJ, et al. Hepatitis C virus nonstructural protein 5a (NS5a) is an RNA-binding protein. J Biol Chem 2005;280:36417-36428.
20. Tellinghuisen TL, Marcotrigiano J, Rice CM. Structure of the zinc-binding domain of an essential component of the hepatitis C virus replicase. Nature 2005;435:374-379.
21. El-Shamy A, Nagano-Fujii M, Sasase N, Imoto S, Kim SR, Hotta H. Sequence variation in hepatitis C virus nonstructural protein 5a predicts clinical outcome of pegylated interferon/ribavirin combination therapy. HEPATOLOGY 2008;48:38-47.

JVI
Journals.ASM.org

Hepatitis C Virus Infection Suppresses GLUT2 Gene Expression via Downregulation of Hepatocyte Nuclear Factor 1α

Chieko Matsui,[a] Ikuo Shoji,[a] Shusaku Kaneda,[a] Imelda Rosalyn Sianipar,[a,b] Lin Deng,[a] and Hak Hotta[a]

Division of Microbiology, Center for Infectious Diseases, Kobe University Graduate School of Medicine, Chuo-ku, Kobe, Hyogo, Japan,[a] and Department of Physiology, Faculty of Medicine, Universitas Indonesia, Jakarta, Indonesia[b]

Hepatitis C virus (HCV) infection causes not only intrahepatic diseases but also extrahepatic manifestations, including type 2 diabetes. We previously reported that HCV replication suppresses cellular glucose uptake by downregulation of cell surface expression of glucose transporter 2 (GLUT2) (D. Kasai et al., J. Hepatol. 50:883–894, 2009). GLUT2 mRNA levels were decreased in both HCV RNA replicon cells and HCV J6/JFH1-infected cells. To elucidate molecular mechanisms of HCV-induced suppression of GLUT2 gene expression, we analyzed transcriptional regulation of the GLUT2 promoter using a series of GLUT2 promoter-luciferase reporter plasmids. HCV-induced suppression of GLUT2 promoter activity was abrogated when the hepatocyte nuclear factor 1α (HNF-1α)-binding motif was deleted from the GLUT2 promoter. HNF-1α mRNA levels were significantly reduced in HCV J6/JFH1-infected cells. Furthermore, HCV infection remarkably decreased HNF-1α protein levels. We assessed the effects of proteasome inhibitor or lysosomal protease inhibitors on the HCV-induced reduction of HNF-1α protein levels. Treatment of HCV-infected cells with a lysosomal protease inhibitor, but not with a proteasome inhibitor, restored HNF-1α protein levels, suggesting that HCV infection promotes lysosomal degradation of HNF-1α protein. Overexpression of NS5A protein enhanced lysosomal degradation of HNF-1α protein and suppressed GLUT2 promoter activity. Immunoprecipitation analyses revealed that the region from amino acids 1 to 126 of the NS5A domain I physically interacts with HNF-1α protein. Taken together, our results suggest that HCV infection suppresses GLUT2 gene expression via downregulation of HNF-1α expression at transcriptional and posttranslational levels. HCV-induced downregulation of HNF-1α expression may play a crucial role in glucose metabolic disorders caused by HCV.

Hepatitis C virus (HCV) is the main cause of chronic hepatitis, liver cirrhosis, and hepatocellular carcinoma. HCV is a single-stranded, positive-sense RNA virus that is classified into the *Flaviviridae* family, *Hepacivirus* genus (21). More than 170 million people worldwide are chronically infected with HCV. The 9.6-kb HCV genome encodes a polyprotein of approximately 3,010 amino acids (aa). The polyprotein is cleaved co- and posttranslationally into at least 10 proteins by viral proteases and cellular signalases: the structural proteins core, E1, E2, and p7 and the nonstructural proteins NS2, NS3, NS4A, NS4B, NS5A, and NS5B (21).

Persistent HCV infection causes not only intrahepatic diseases but also extrahepatic manifestations, such as type 2 diabetes. Clinical and experimental data suggest that HCV infection is an additional risk factor for the development of diabetes (26, 29, 30). HCV-related glucose metabolic changes and insulin resistance have significant clinical consequences, such as accelerated fibrogenesis, reduced virological response to alpha interferon (IFN-α)-based therapy, and increased incidence of hepatocellular carcinoma (29). Therefore, the molecular mechanism of HCV-related diabetes needs to be clarified.

We have sought to identify a novel mechanism of HCV-induced diabetes. We previously demonstrated that HCV suppresses hepatocytic glucose uptake through downregulation of cell surface expression of glucose transporter 2 (GLUT2) in a human hepatoma cell line (19). The uptake of glucose into cells is conducted by facilitative glucose carriers, i.e., glucose transporters (GLUTs). GLUTs are integral membrane proteins that contain 12 membrane-spanning helices. To date, a total of 14 isoforms have been identified in the GLUT family (24). GLUT2 is expressed in the liver, pancreatic β-cells, hypothalamic glial cells, retina, and enterocytes. Glucose is transported into hepatocytes by GLUT2 (34). We previously reported that GLUT2 expression was reduced in hepatocytes obtained from HCV-infected patients (19). We also demonstrated that GLUT2 mRNA levels were lower in HCV replicon cells and in HCV J6/JFH1-infected cells than in the control cells. GLUT2 promoter activity was suppressed in HCV-replicating cells. However, the molecular mechanism of HCV-induced suppression of GLUT2 gene expression remains to be elucidated.

In the present study, we aimed to clarify molecular mechanisms of HCV-induced suppression of GLUT2 gene expression. We analyzed transcriptional regulation of the GLUT2 promoter in HCV replicon cells. We demonstrate that HCV infection downregulates hepatocyte nuclear factor 1α (HNF-1α) expression at both transcriptional and posttranslational levels, resulting in suppression of GLUT2 promoter. We propose that HCV-induced downregulation of HNF-1α may play a crucial role in glucose metabolic disorders caused by HCV.

MATERIALS AND METHODS

Cell culture. The human hepatoma cell line Huh-7.5 (4) was kindly provided by Charles M. Rice (The Rockefeller University, New York, NY).

Received 8 June 2012 Accepted 11 September 2012
Published ahead of print 19 September 2012
Address correspondence to Hak Hotta, hotta@kobe-u.ac.jp, or Ikuo Shoji, ishoji@med.kobe-u.ac.jp.

doi:10.1128/JVI.01418-12

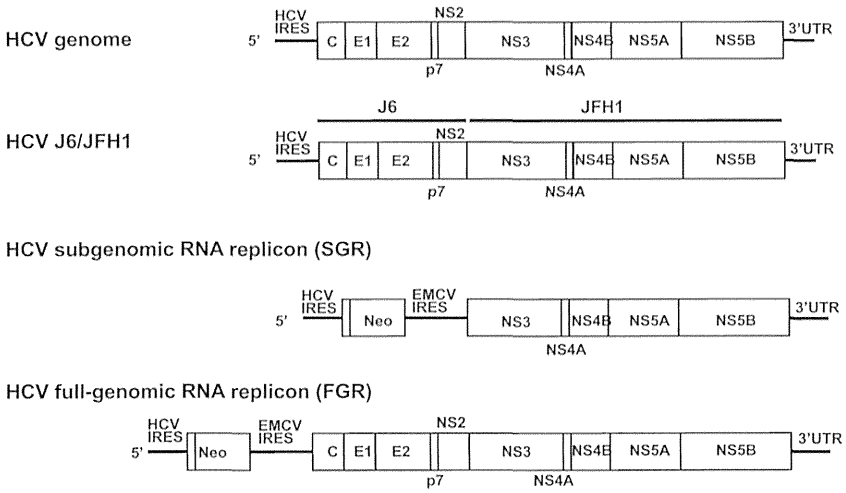

FIG 1 The HCV genome, chimeric HCV J6/JFH1, and the HCV RNA replicons. Schematic diagrams of the HCV genome, the chimeric HCV J6/JFH1 genome, SGR, and FGR are shown. IRES, internal ribosome entry site; EMCV, encephalomyocarditis virus; Neo, neomycin resistance gene.

Cells were cultured in Dulbecco's modified Eagle's medium (DMEM) (high glucose) with L-glutamine (Wako, Osaka, Japan) supplemented with 50 IU/ml penicillin, 50 μg/ml streptomycin (Gibco, NY), 10% heat-inactivated fetal bovine serum (Biowest, France), and 0.1 mM nonessential amino acids (Invitrogen, NY) at 37°C in a 5% CO_2 incubator. Cells were transfected with plasmid DNA using FuGENE 6 transfection reagents (Promega, Madison, WI).

Huh-7.5 cells stably harboring an HCV-1b subgenomic RNA replicon (SGR) were prepared as described previously (18), using pFK5B/2884Gly (a kind gift from R. Bartenschlager, University of Heidelberg, Heidelberg, Germany). The SGR cells express the genomic region from NS3 to NS5B of the HCV Con1 strain (19) (Fig. 1). Cells harboring a full-genome HCV-1b RNA replicon (FGR) derived from Con1 (27) or pON/C-5B (17, 19) (a kind gift from N. Kato, Okayama University, Okayama, Japan) were also used. The FGR cells express all of the HCV proteins (the region ranging from the core protein to NS5B).

The pFL-J6/JFH1 plasmid that encodes the entire viral genome of a chimeric strain of HCV-2a, J6/JFH1 (23), was kindly provided by Charles M. Rice. The HCV genome RNA was synthesized *in vitro* using pFL-J6/JFH1 as a template and was transfected into Huh-7.5 cells by electroporation (6, 9, 23, 37). The virus produced in the culture supernatant was used for infection experiments (6).

Cells were treated with 1,000 IU/ml of IFN-α (Sigma, St. Louis, MO) for 10 days to eliminate HCV replication (19).

Luciferase reporter assay. We constructed the human GLUT2 promoter-luciferase reporter plasmid by cloning a 1.6-kb genomic fragment that encompasses the human GLUT2 promoter region from −1291 to +308, yielding pGLUT2(−1291/+308)-Luc (2, 19), into the pGL4 vector plasmid (Promega). The pGLUT2(−1291/+308)-Luc construct contains a 1,291-bp fragment of the human GLUT2 promoter upstream of the minimal promoter and the coding sequence of the *Photinus pyralis* (firefly) luciferase. We also used seven different GLUT2 promoter-luciferase reporter plasmids, i.e., pGLUT2(−1193/+308)-Luc, pGLUT2 (−1155/+308)-Luc, pGLUT2(−1100/+308)-Luc, pGLUT2(−1030/+308)-Luc, pGLUT2(−206/+308)-Luc, pGLUT2(+29/+308)-Luc, and pGLUT2(+126/+308)-Luc, which lack the binding sequence of the CCAAT/enhancer binding site (C/EBP), cyclic AMP (cAMP) response element (CRE), AP-1 binding site, HNF-1α binding site, CAAT box, TATA-like motif, and transcriptional initiation, respectively (Fig. 2A). The reporter plasmid pRL-CMV-*Renilla* (where CMV is cytomegalovirus) (Promega) was used as an internal control. Cells were transfected with each pGLUT2-Luc construct together with pRL-CMV-*Renilla*. At 48 h after transfection, samples were harvested and assayed for luciferase activity. The luciferase assays were performed using a dual-luciferase reporter assay system (Promega). Luciferase activity was measured by a Lumat LB 9501 instrument (Berthold Technologies GmbH & Co., Bad Wildbad, Germany). Firefly luciferase activity was normalized to *Renilla* luciferase activity for each sample. The number of relative light units (RLU) of the SGR cells or FGR cells transfected with each reporter plasmid is expressed as a ratio of the number of Huh-7.5 cells transfected with each reporter plasmid.

Expression plasmids. Expression plasmids for core protein, p7, NS2, NS3, NS4A, NS4B, NS5A, and NS5B were described previously (9, 10, 18). To express E1 and E2 (E1/E2), the cDNA fragment of nucleotides (nt) 825 to 2676 derived from the HCV Con1 strain was amplified by PCR using the plasmid pFKI389neo/core-3′/Con1 (a kind gift from R. Bartenschlager) as a template. Specific primers used for PCR were as follows: sense primer, 5′-CCAGTGTGGTGAATTCAC CATGGTGAACTATGCAACAGGGAA-3′; antisense primer, 5′-CGAAG GGCCCTCTAGAGATGTACCAGGCAGCACAGA-3′. To express NS3 and NS4A (NS3/4A), the cDNA fragment of nt 3420 to 5474 derived from the HCV Con1 strain was amplified by PCR. Specific primers were as follows: sense primer, 5′-CCAGTGTGGTGAATTCACCATGGCGCCTA TTACGGCCTACTC-3′; antisense primer, 5′-CGAAGGGCCCTCTAGA GCACTCTTCCATCTCATCGAA-3′. These amplified PCR products were purified, and each of them was inserted into the EcoRI-XbaI site of pEF1/myc-His A (Invitrogen) using an In-Fusion HD-Cloning kit (Clontech, Mountain View, CA). To express a series of NS5A deletion mutants as hemagglutinin (HA)-tagged proteins, each fragment was amplified by PCR and cloned into the NotI site of pCAG-HA. pEF1A-NS5A (Con1)-myc-His was used as a template (18). The primer sequences used in this study are available from the authors upon request. The sequences of the inserts were extensively verified by sequencing (Operon biotechnology, Tokyo, Japan). The plasmids pEF1A-NS5A(1–126)-myc-His, consisting of residues 1 to 126 in NS5A, and pEF1A-NS5A(1–147)-myc-His were described previously (18).

Antibodies. The mouse monoclonal antibodies (MAbs) used in this study were anti-FLAG (M2) MAb (F-3165; Sigma), anti-NS5A MAb (MAB8694; Millipore), anti-core protein MAb (2H9) (37), and anti-glyceraldehyde-3-phosphate dehydrogenase (GAPDH) MAb (MAB374; Millipore). Polyclonal antibodies (PAbs) used in this study were anti-HNF-1α rabbit PAb (sc-8986; Santa Cruz Biotechnology), anti-HNF-1α goat PAb (sc-6548; Santa Cruz Biotechnology), anti-NS5B goat PAb (sc-17532; Santa Cruz Biotechnology), anti-NS3 rabbit PAb (described elsewhere), and anti-actin goat PAb (C-11; Santa Cruz Biotechnology). Horseradish peroxidase (HRP)-conjugated anti-mouse IgG antibody

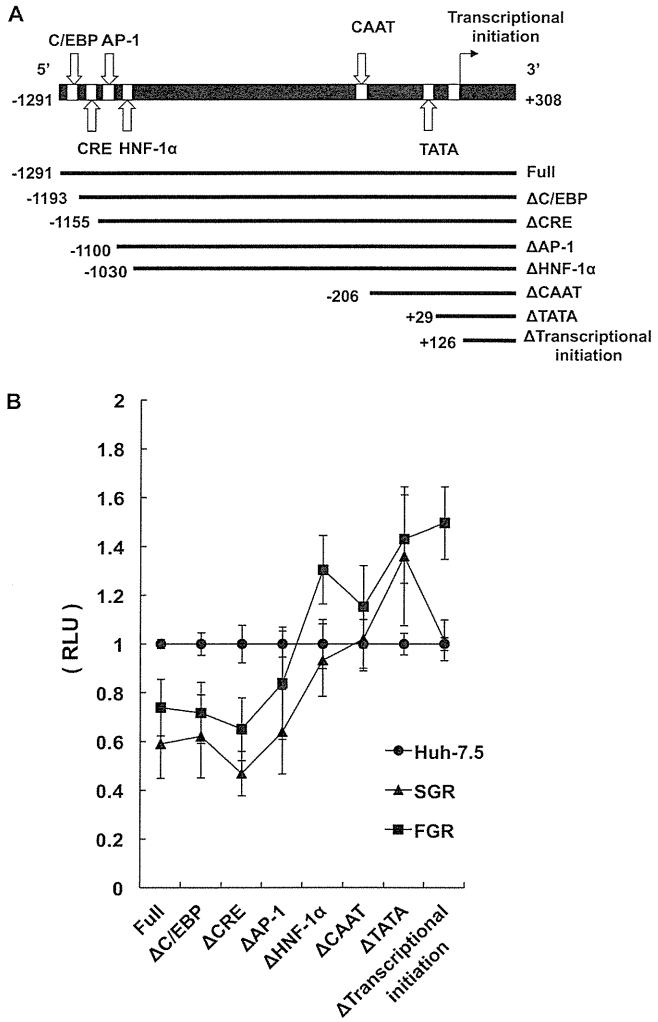

FIG 2 HNF-1α-binding site is important for HCV-induced suppression of GLUT2 promoter. (A) A series of constructs in which genomic GLUT2 promoter DNA fragments were fused to a promoterless firefly luciferase gene of the pGL4 vector were generated with the 3′ end always terminating at bases +308 from transcriptional start site. The 5′ ends began at bases −1291, −1193, −1155, −1100, −1030, −206, +29, and +126 The regions that represent potential binding sites for transcription factors are shown, including a CCAAT/enhancer binding site (C/EBP), cAMP response element (CRE), AP-1 binding site, HNF-1α binding site, CAAT box, and TATA-like motif. The nucleotide at the beginning of the construct is indicated. (B) Huh-7.5 cells, SGR cells, and FGR cells (2.5×10^5 cells/six-well plate) were transfected with each GLUT2 plasmid (0.5 μg) together with pRL-CMV-*Renilla* (25 ng). pRL-CMV-*Renilla* was used as an internal control. At 48 h posttransfection, cells were harvested and assayed for luciferase activities using a dual-luciferase reporter assay system. RLU is expressed as a ratio of the Huh-7.5 cells transfected with each reporter plasmid.

(Cell signaling), HRP-conjugated donkey anti-goat IgG (Santa Cruz Biotechnology), and HRP-conjugated anti-rabbit IgG (Cell signaling) were used as secondary antibodies.

Real-time quantitative reverse transcription-PCR (RT-PCR). Total cellular RNA was isolated using RNAiso reagent (TaKaRa Bio, Kyoto, Japan), and cDNA was generated using a QuantiTect Reverse Transcription system (Qiagen, Valencia, CA). Real-time quantitative PCR was performed using SYBR Premix *Ex Taq* (TaKaRa Bio) with SYBR green chemistry on an ABI Prism 7000 system (Applied Biosystems, Foster, CA), as described previously (11, 19). The β-glucronidase (GUS) gene was used as an internal control. The primers used for real-time PCR are as follows: for HNF-1α (NM_000545), 5′-AGCTACCAACCAAGAAGGGGC-3′ (nt 601 to 621) and 5′-TGACGAGGTTGGAGCCCAGCC-3′ (nt 801 to 781); HNF-1β (NM_000458), 5′-GTTACATGCAGCAACACAACA-3′ (nt 600 to 620) and 5′-TCATATTTCCAGAACTCTGGA-3′ (nt 801 to 782); GUS (NM_000181), 5′-ATCAAAAACGCAGAAAATACG-3′ (nt 1797 to 1817) and 5′-ACGCAGGTGGTATCAGTCTTG-3′ (nt 2034 to 2014).

Immunoblot analysis. Immunoblot analysis was performed essentially as described previously (9, 33). The cell lysates were separated by 8% sodium dodecyl sulfate-polyacrylamide gel electrophoresis (SDS-PAGE) and transferred to polyvinylidene difluoride membrane (Millipore Corp., Billerica, MA). The membranes were incubated with primary antibody, followed by incubation with peroxidase-conjugated secondary antibody. The positive bands were visualized using ECL Western blotting detection reagents (GE Healthcare, Buckinghamshire, United Kingdom). To detect endogenous HNF-1α protein, ECL Plus Western blotting detection reagents were used (GE Healthcare).

Immunoprecipitation. Cultured cells were lysed with a buffer containing 150 mM NaCl, 20 mM Tris-HCl (pH 7.4), 0.1% SDS, 1% NP-40, and Complete protease inhibitor cocktail (Roche Diagnostics, Indianapolis, IN). The lysate was centrifuged at 12,000 × *g* for 20 min at 4°C, and the supernatant was immunoprecipitated with appropriate antibodies. Immunoprecipitation was performed as described previously (10). Briefly, the cell lysates were immunoprecipitated with control IgG and Dynabeads protein A (Invitrogen) and incubated with appropriate antibodies at 4°C overnight. After being washed with the washing buffer (0.1 M Na-phosphate buffer, pH 7.4) five times, the immunoprecipitates were analyzed by immunoblotting.

Statistical analysis. Results were expressed as means ± standard errors of the means (SEM). Statistical significance was evaluated by analysis of variance (ANOVA), and statistical significance was defined as a P value of <0.05.

RESULTS

HNF-1α-binding site is important for HCV-induced suppression of GLUT2 promoter. To gain an insight into potential regulatory sequences involved in HCV-induced suppression of GLUT2 gene transcription, a 1.6-kb genomic fragment that encompasses the human GLUT2 promoter (−1291 to +308) and a series of deletion mutants were analyzed (Fig. 2A). The ability of the upstream region of the GLUT2 gene to function as a promoter was assessed by its capacity to drive the expression of a luciferase reporter gene. GLUT2 promoter activity was assessed by measuring luciferase activity of the cell extracts derived from transiently transfected Huh-7.5 cells, SGR cells, and FGR cells. As shown in Fig. 2B, a deletion of the promoter sequence to −1100 [pGLUT2(−1100/+308)-Luc [ΔAP-1]] showed lower luciferase activities in HCV replicon cells than in the control cells. Successive removal of nucleotides from −1100 to −1030 completely or almost completely abolished the suppression of the luciferase activity in both FGR and SGR cells, suggesting that the HNF-1α-binding site is important for HCV-induced suppression of GLUT2 promoter.

HCV infection reduces HNF-1α mRNA levels. It is worth noting that HNF-1α is known to play a crucial role in diabetes. Mutations in the HNF-1α gene have been reported to cause a monogenic form of diabetes mellitus with autosomal dominant inheritance, termed maturity onset diabetes of the young 3 (MODY3) (25, 40). Cha et al. (7) reported that HNF-1α functions as a transcriptional transactivator in human GLUT2 gene expression in a human hepatoma cell line. These findings motivated us to further investigate a role of HNF-1α in HCV-induced glucose metabolic disorders in a human hepatoma cell line. To determine

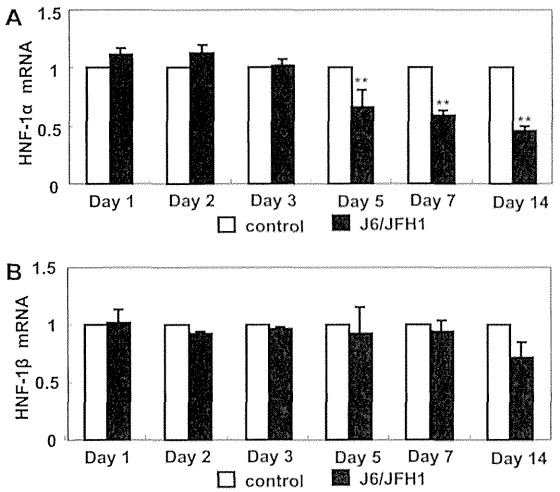

FIG 3 Quantitative RT-PCR analysis of mRNA for HNF-1α and HNF-1β in HCV J6/JFH1-infected cells. Huh-7.5 cells (2.5×10^5 cells/six-well plate) were infected with HCV J6/JFH1 at a multiplicity of infection of 2. Cells were cultured and harvested at the indicated times. Total RNA was extracted, and the levels of HNF-1α mRNA and HNF-1β mRNA were determined by quantitative RT-PCR. Mock-infected cells served as negative controls. **, $P < 0.01$, compared with mock-infected cells.

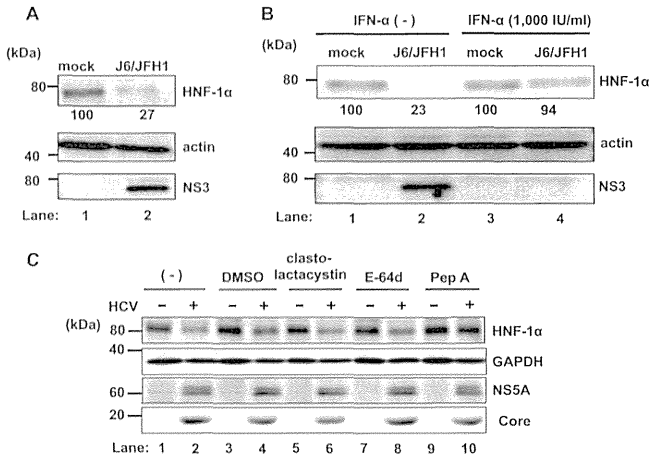

FIG 4 HCV infection induces lysosomal degradation of HNF-1α protein. (A) HCV infection decreased the levels of HNF-1α protein in Huh-7.5 cells. Huh-7.5 cells (2.5×10^5 cells/six-well plate) were infected with HCV J6/JFH1 at a multiplicity of infection of 2. Cells were cultured and harvested at 5 days postinfection. Cells were analyzed by immunoblotting with anti-HNF-1α, anti-NS3, and anti-actin antibodies. The level of actin served as a loading control. The relative levels of protein expression were quantitated by densitometry and are indicated below the respective lanes. (B) HCV-induced downregulation of HNF-1α protein was restored by treatment of the cells with IFN-α. Huh-7.5 cells were plated at 2.5×10^5 cells/six-well plate and cultured for 12 h. The cells were infected with HCV J6/JFH1 at a multiplicity of infection of 2 and cultured for 5 days. The cells were replated at 2.5×10^5 cells/six-well plate and cultured in complete DMEM with or without 1,000 IU/ml IFN-α for 10 days to eliminate HCV. The cells cultured in DMEM without IFN-α served as negative controls. (C) HCV-induced reduction of HNF-1α protein was restored by treatment of the cells with lysosomal protease inhibitor. Huh-7.5 cells were plated at 2.0×10^5 cells/six-well plate and cultured for 12 h. At 5 days postinfection, proteasome inhibitor (30 μM clasto-lactacystin β-lactone) or lysosomal protease inhibitors (40 μM E-64d and 20 μM pepstatin A) were administered to the cells. Cells were cultured for 12 h, harvested, and analyzed by immunoblotting as indicated. The level of GAPDH served as a loading control. DMSO, dimethyl sulfoxide; PepA, pepstatin A.

whether HCV infection suppresses HNF-1α mRNA expression, we quantified mRNA levels of HNF-1α and HNF-1β in HCV J6/JFH1-infected cells and in mock-infected cells by real-time RT-PCR. HNF-1α mRNA levels were significantly reduced in HCV J6/JFH1-infected cells from 5 days postinfection (dpi) to 14 dpi (Fig. 3A). On the other hand, HNF-1β mRNA levels remained unchanged until 14 dpi (Fig. 3B). These results suggest that HCV infection specifically downregulates HNF-1α mRNA expression.

HCV infection reduces HNF-1α protein levels. To determine whether HCV infection reduces HNF-1α protein levels, endogenous HNF-1α protein levels were examined by immunoblot analysis. The HNF-1α protein level was much lower in J6/JFH1-infected cells than in the mock-infected control (Fig. 4A, upper panel, lane 2). To determine whether HCV infection is specifically involved in reduction of HNF-1α protein, we eliminated HCV by treatment of the cells with IFN-α (Fig. 4B, lower panel, compare lane 2 with lane 4). Upon elimination of HCV, the HNF-1α protein expression level recovered to the level of the mock-infected control (Fig. 4B, upper panel, compare lane 2 with lane 4). These results suggest that HCV infection specifically reduces HNF-1α protein levels.

HCV-induced reduction of HNF-1α protein is restored by treatment of the cells with a lysosomal protease inhibitor. As shown in Fig. 3A, HNF-1α mRNA levels in HCV J6/JFH1-infected cells decreased slowly at day 5 postinfection. One possible explanation is that suppression of HNF-1α mRNA is an indirect effect caused by HCV infection. The degree of the reduction of the HNF-1α protein was larger than that of HNF-1α mRNA (Fig. 4A), suggesting the involvement of protein degradation in reduction of HNF-1α protein levels. To determine whether protein degradation is involved in HCV-induced reduction of HNF-1α protein, we assessed the role of proteasome or lysosome proteases in the reduction of HNF-1α protein. We treated the cells with a proteasome inhibitor, clasto-lactacystin β-lactone, or lysosome protease inhibitors E-64d and pepstatin A. Clasto-lactacystin β-lactone had no effect on the levels of HNF-1α protein (Fig. 4C, upper panel, lane 6). This result suggests that proteasome is not involved in the reduction of HNF-1α protein. E-64d is a cysteine protease inhibitor, and pepstatin A is an aspartic protease inhibitor. Pepstatin A, but not E-64d, restored the levels of HNF-1α protein (Fig. 4C, upper panel, lanes 10 and 8). These results suggest that a lysosomal protease, such as an aspartic protease, is involved in HCV-induced reduction of HNF-1α protein.

Overexpression of NS5A protein suppresses GLUT2 promoter activity. To determine which HCV protein is involved in the suppression of GLUT2 promoter, we examined the effects of transient expression of HCV proteins on GLUT2 promoter activity. Huh-7.5 cells were cotransfected with each HCV protein expression plasmid together with the GLUT2 promoter-luciferase plasmid. The pRL-CMV-*Renilla* plasmid was cotransfected as an internal control. At 48 h posttransfection, cells were harvested and assayed for luciferase activity. As shown in Fig. 5A, overexpression of the NS5A expression plasmid significantly reduced GLUT2 promoter activity. On the other hand, other HCV protein expression plasmids failed to suppress GLUT2 promoter activity (Fig. 5A, left and right panels). These results suggest that NS5A protein is involved in the suppression of GLUT2 promoter activity.

Overexpression of NS5A protein reduces the levels of endogenous HNF-1α protein. To investigate a role of NS5A in the sup-

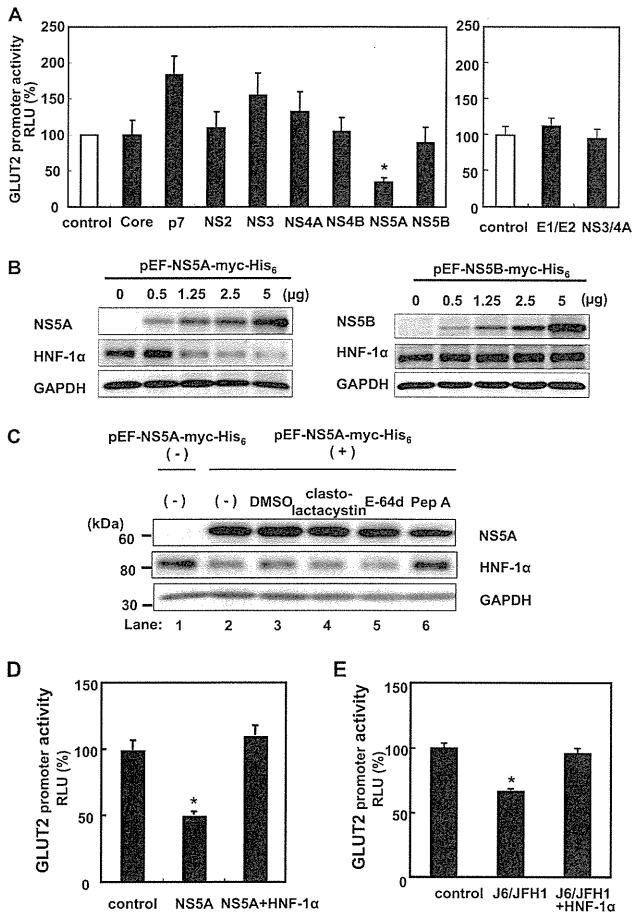

FIG 5 HCV NS5A protein is involved in suppression of GLUT2 promoter activity and lysosomal degradation of HNF-1α protein. (A) Huh-7.5 cells were plated at 1×10^5 cells/12-well plate. After cells were cultured for 12 h, cells were cotransfected with each HCV protein plasmid (0.5 μg), the human GLUT2 promoter reporter plasmid (0.5 μg), and pRL-CMV-*Renilla* (25 ng). pRL-CMV-*Renilla* was used as an internal control. At 48 h posttransfection, cells were harvested. Luciferase assays were performed by using a dual-luciferase reporter assay system. (B) Huh-7.5 cells were plated at 4×10^5 cells/six-well plate and cultured for 12 h. Cells were transfected with increasing amounts of either NS5A plasmid or NS5B plasmid as indicated. At 48 h posttransfection, cells were harvested. Whole-cell lysates were analyzed by immunoblotting with anti-HNF-1α, anti-NS5A, and anti-NS5B antibodies. The level of GAPDH served as a loading control. (C) Huh-7.5 cells (2.5×10^5 cells/six-well plate) were transfected with pEF1A-NS5A-myc-His_6. At 2 days posttransfection, proteasome inhibitor (30 μM clasto-lactacystin β-lactone) or lysosomal enzyme inhibitors (40 μM E-64d and 20 μM pepstatin A) were administered to the cells. Cells were cultured for 12 h and harvested, and the levels of endogenous HNF-1α protein were analyzed by immunoblotting with anti-HNF-1α goat PAb. The level of GAPDH served as a loading control. (D) Huh-7.5 cells (1.0×10^5 cells/12-well plate) were transfected with the human GLUT2 promoter reporter plasmid (0.5 μg) and pRL-CMV-*Renilla* (25 ng). The plasmid pEF1A/myc-His (0.5 μg) was cotransfected to the control cells. Cells were transfected with the plasmid pEF1A-NS5A-myc-His (0.5 μg) together with either empty plasmid pCMV4 (10 ng) or pCMV-HNF-1α (10 ng). At 48 h posttransfection, cells were harvested. Luciferase assays were performed by using a dual-luciferase reporter assay system. *, $P < 0.05$, compared with control. (E) Huh-7.5 cells (1.2×10^6 cells /10 cm-dish) were infected with HCV J6/JFH1 at a multiplicity of infection of 2 and cultured for 5 days. At day 5 postinfection, cells were plated at 1.0×10^5 cells/12-well plate and cultured for 12 h. Mock-infected cells were plated similarly. Cells were transfected with the human GLUT2 promoter reporter plasmid (0.5 μg) and pRL-CMV-*Renilla* (25 ng) together with either empty plasmid pCMV4 or pCMV-HNF-1α, cultured for 48 h, and harvested. Luciferase assays were performed by using a dual-luciferase reporter assay system. *, $P < 0.05$, compared with control.

pression of the GLUT2 promoter, we examined the effect of NS5A protein on the levels of endogenous HNF-1α protein. Huh-7.5 cells were transfected with increasing amounts of either an NS5A expression plasmid or NS5B expression plasmid. At 48 h post-transfection, cells were harvested, and the levels of endogenous HNF-1α protein were analyzed by immunoblot analysis. To detect endogenous HNF-1α protein, highly sensitive Western blotting detection reagents (ECL Plus Western blotting detection reagents) were used. Overexpression of NS5A (Fig. 5B, left panel) but not NS5B (Fig. 5B, right panel) significantly reduced endogenous HNF-1α protein. These results suggest that NS5A protein specifically reduces endogenous HNF-1α protein levels.

To determine if NS5A-dependent reduction of HNF-1α protein is due to lysosomal degradation, we treated the cells with lysosome protease inhibitors. Pepstatin A, but not E-64d, recovered the levels of HNF-1α protein (Fig. 5C, middle panel, lanes 5 and 6), which is consistent with the results found in HCV-infected cells. These results suggest that NS5A is responsible for HCV-induced lysosomal degradation of HNF-1α protein. Taken together, our results suggest that HCV infection suppresses GLUT2 promoter activity via NS5A-dependent lysosomal degradation of HNF-1α protein.

To verify a role of HNF-1α in the HCV-induced suppression of GLUT2 promoter activity, we examined the effects of ectopic expression of HNF-1α on GLUT2 promoter activity in NS5A-transfected cells as well as in HCV J6/JFH1-infected cells. As shown in Fig. 5D, overexpression of NS5A decreased GLUT2 promoter activity, and ectopic expression of HNF-1α restored GLUT2 promoter activity (Fig. 5D). Moreover, HCV J6/JFH1 infection significantly decreased GLUT2 promoter activity, and ectopic expression of HNF-1α restored GLUT2 promoter activity (Fig. 5E). These results are consistent with the notion that HNF-1α protein is a key regulator for HCV-induced suppression of GLUT2 promoter activity.

NS5A protein interacts with HNF-1α protein in Huh-7.5 cells and in FGR Con1 cells. It was previously reported that *in vitro* translated HNF-1 protein was pulled down with glutathione *S*-transferase (GST)-NS5A protein (32). To determine whether NS5A physically interacts with HNF-1α protein in cultured cells, Huh-7.5 cells were cotransfected with each FLAG-tagged NS5A expression plasmid together with the HNF-1α expression plasmid. Immunoprecipitation analysis revealed that HNF-1α protein was coimmunoprecipitated with FLAG-NS5A protein using anti-FLAG MAb (Fig. 6A, third blot, lane 8). No band was detected using control IgG for immunoprecipitation (Fig. 6A, third blot, lane 7). Conversely, immunoprecipitation analysis revealed that NS5A protein was coimmunoprecipitated with HNF-1α protein using anti-HNF-1α rabbit PAb (Fig. 6B, fourth blot, lane 8). Moreover, NS5A protein was coimmunoprecipitated with endogenous HNF-1α protein (Fig. 6B, fourth blot, lane 6), suggesting that NS5A protein indeed interacts with HNF-1α protein.

To confirm that HCV NS5A protein can interact with HNF-1α protein in HCV-replicating cells, we performed immunoprecipitation analysis using FGR Con1 (RCYM1) cells. NS5A protein was coimmunoprecipitated with endogenous HNF-1α protein (Fig. 6C, fourth blot, lane 2). Transfection of HNF-1α protein increased the level of coimmunoprecipitated NS5A protein (Fig. 6C, fourth blot, lane 4), suggesting that HCV NS5A protein indeed interacts with HNF-1α protein in HCV-replicating cells.

HNF-1α binds domain I of NS5A protein. To map the HNF-

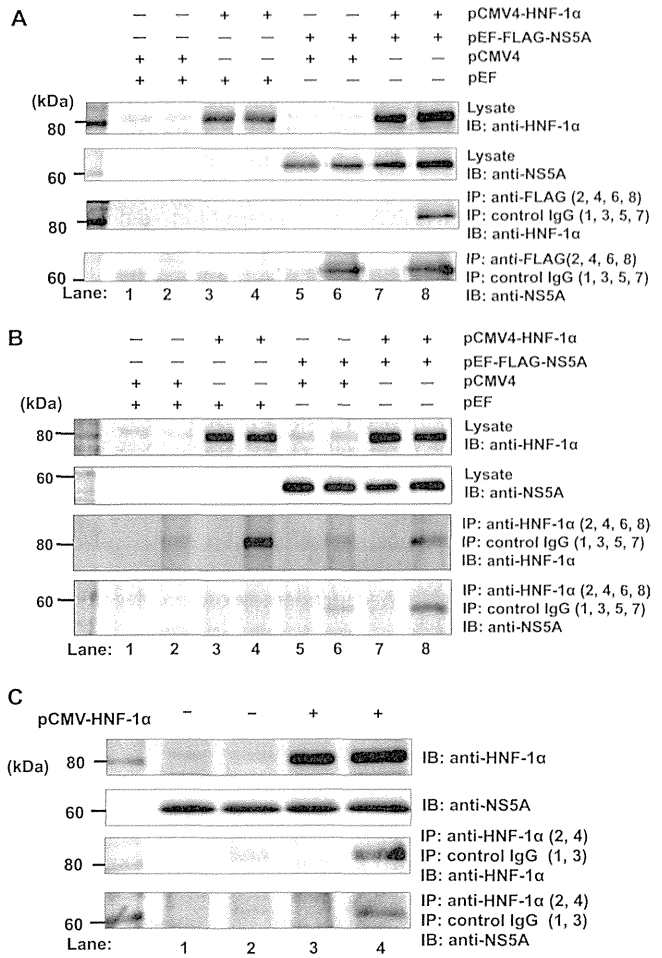

FIG 6 NS5A protein interacts with HNF-1α protein. (A) Huh-7.5 cells were plated at 1.2×10^6 cells/10-cm dish and cultured for 12 h. Cells were transfected with plasmids as indicated. At 48 h after transfection, cells were harvested. Cell lysates were immunoprecipitated with either anti-FLAG mouse MAb (lanes 2, 4, 6, and 8) or control IgG (lanes 1, 3, 5, and 7), and bound proteins were immunoblotted with anti-HNF-1α rabbit PAb (third blot) or anti-NS5A mouse MAb (fourth blot). Protein expression of HNF-1α or FLAG-NS5A was confirmed using the same cell lysates by immunoblotting with either anti-HNF-1α rabbit PAb (first blot) or anti-NS5A mouse MAb (second blot). (B) Cell lysates were immunoprecipitated with either anti-HNF-1α rabbit PAb (lanes 2, 4, 6, and 8) or control IgG (lanes 1, 3, 5, and 7), and bound proteins were immunoblotted with either anti-HNF-1α rabbit PAb (third blot) and anti-NS5A mouse MAb (fourth blot). (C) Full-genome replicon Con1 (RCYM1) cells were plated at 1.2×10^6 cells/10-cm plate and transfected with or without pCMV-HNF-1α plasmid and cultured for 48 h. Cells were harvested and assayed for immunoprecipitation with anti-HNF-1α rabbit PAb (lanes 2 and 4) or control IgG (lanes 1 and 3). Bound proteins were immunoblotted with anti-HNF-1α goat PAb (third blot) or anti-NS5A mouse MAb (fourth blot). Input samples were immunoblotted with either anti-HNF-1α PAb (first blot) or anti-NS5A MAb (second blot). IP, immunoprecipitation; IB, immunoblotting.

1α-binding site on NS5A protein, coimmunoprecipitation analyses were performed. By use of a panel of NS5A deletion mutants (Fig. 7A), FLAG-HNF-1α protein was found to coimmunoprecipitate with all of the HA-NS5A proteins except HA-NS5A consisting of aa 357 to 447 [HA-NS5A(357–447), HA-NS5A(250–447), or HA-NS5A(214–447) (Fig. 7B, lower left panel). These results suggest that domain I of NS5A consisting of aa 1 to 213 is important for HNF-1α binding. FLAG-HNF-1α protein was also found to coimmunoprecipitate with NS5A(1–126)-myc-His_6 and NS5A(1–147)-myc-His_6. These data led to the conclusion that the HNF-1α-binding domain of NS5A protein was aa 1 to 126.

DISCUSSION

In this study, we aimed to clarify molecular mechanisms of HCV-induced suppression of GLUT2 gene expression. The reporter assays of the human GLUT2 promoter suggest that the HNF-1α-binding site is crucial for HCV-induced suppression of GLUT2 promoter activity (Fig. 2). HCV infection significantly reduced the levels of HNF-1α mRNA (Fig. 3A). Moreover, HCV infection remarkably decreased HNF-1α protein levels (Fig. 4A). Our results suggest that HCV infection suppresses GLUT2 gene expression via NS5A-mediated lysosomal degradation of HNF-1α protein (Fig. 5). Immunoprecipitation analyses revealed that NS5A protein physically interacts with HNF-1α protein (Fig. 6) and that domain I of NS5A is important for HNF-1α binding (Fig. 7). Taken together, our results suggest that HCV infection suppresses GLUT2 transcription via downregulation of HNF-1α expression at both transcriptional and translational levels (Fig. 8).

We demonstrated that HNF-1α protein levels were greatly reduced compared to the reduced levels of HNF-1α mRNA. We demonstrated that pepstatin A, but not E64-d, restored the levels of HNF-1α protein, suggesting that an aspartic protease is involved in the degradation of HNF-1α protein. Pepstatin A is widely used for investigation of autophagy and lysosomal degradation. Further studies are needed to elucidate how HCV induces lysosomal degradation of HNF-1α protein and how HNF-1α protein is selectively downregulated by HCV infection. Our data suggest that the HCV NS5A protein is responsible for the HCV-induced degradation of HNF-1α protein. Using a panel of NS5A deletion mutants, we demonstrated that domain I of NS5A is important for association with HNF-1α protein. NS5A domain I is relatively conserved among HCV genotypes compared to domains II and III, suggesting that NS5A–HNF-1α interaction is common to all the HCV genotypes. Domain I coordinates a single zinc atom per protein molecule and is essential for HCV RNA replication (35). The crystal structure of NS5A domain I revealed the presence of a zinc coordination motif and a C-terminal disulfide bond (36). NS5A domain I was found to bind many host proteins, RNA, and membranes (16). It is possible that physical interaction between NS5A protein and HNF-1α protein is important for selective degradation of HNF-1α protein. One possible mechanism is that NS5A protein may recruit HNF-1α protein to the lysosome. Further study is necessary to test this possibility.

We observed that deletion of the GLUT2 transcriptional start site enhances expression of the GLUT2 reporter in FGR cells (Fig. 2B). Cha et al. (7) previously reported that deletion down to nucleotide +73 of the GLUT2 promoter resulted in a marked increase and that further deletion to nucleotide +188 caused a drastic decrease in luciferase activity, indicating the presence of negative- and positive-regulator elements in the 5′ untranslated region. The role of these elements in HCV-infected cells remains to be elucidated.

We demonstrated that HCV J6/JFH1 infection reduced the HNF-1α mRNA level and HNF-1α protein level. Our results contradict an earlier report (32) demonstrating that expression of HNF-1 mRNA was increased in subgenomic replicon Huh.8 cells (3). We observed downregulation of HNF-1α mRNA and

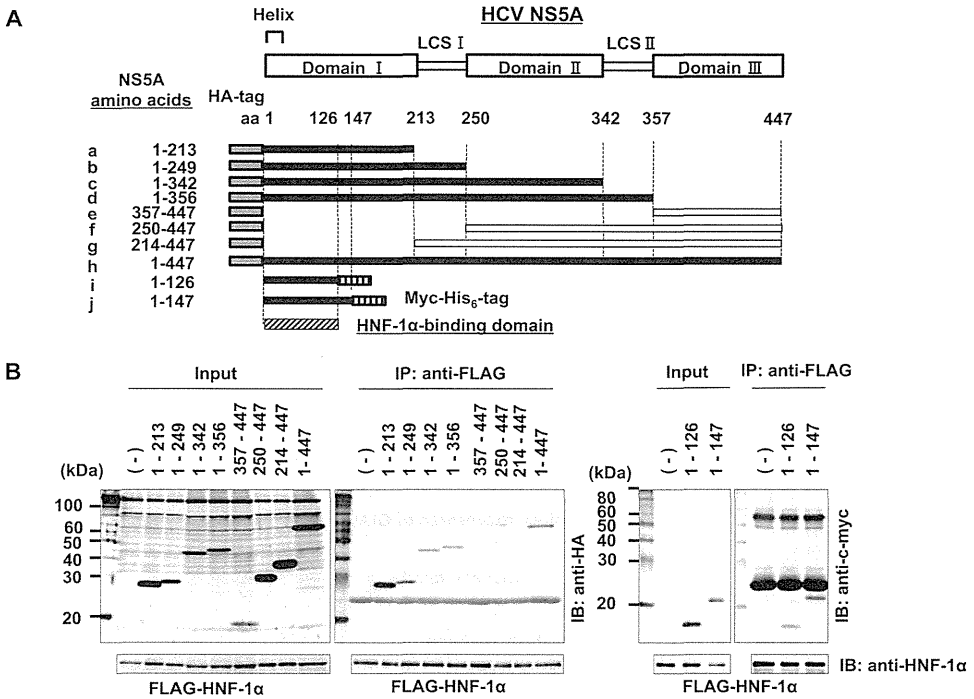

FIG 7 Mapping of the HNF-1α-binding domain for NS5A protein. (A) Schematic representation of the hepatitis C virus NS5A protein. NS5A consists of three domains (domains I, II, and III) with domains separated by low-complexity sequences (LCS I and II). The position of the amino-terminal amphipathic helix membrane anchor is shown (labeled helix). The NS5A deletion mutants (a to j) contain the NS5A amino acids indicated to the left. Each NS5A deletion mutant contains either HA tag in the N terminus (a to h) or myc-His_6 tag in the C terminus (i and j). The gray region of each represents the HA tag sequence. The lattice region of each represents the myc-His_6 tag (i and j). Closed boxes represent proteins that are bound specifically to HNF-1α protein, and open boxes represent those that are not bound. (B) Huh-7.5 cells were transfected with each NS5A mutant plasmid together with a FLAG-HNF-1α expression plasmid. At 48 h posttransfection, cells were harvested, and cell lysates were immunoprecipitated with anti-FLAG beads. Input samples and immunoprecipitated samples were immunoblotted with anti-HA MAb (two left panels, top), anti-c-myc MAb (two right panels, top), or anti-HNF-1α PAb (all panels, bottom).

HNF-1α protein in SGR cells as well as in FGR cells (data not shown). We also demonstrated that the ectopic expression of NS5A protein decreased the endogenous HNF-1α protein level. The reasons for these discrepancies remain to be elucidated.

We along with other groups previously reported that HCV NS5A protein is involved in mitochondrial reactive oxygen species (ROS) production (11, 13, 38). Mitochondrial ROS generation is known to induce the autophagy pathway (22) and lysosomal membrane permeabilization (8). Therefore, it is necessary to determine whether NS5A-induced ROS production enhances autophagic degradation or lysosomal membrane permeabilization. Several groups have reported that autophagy vesicles accumulate in HCV-infected cells and that autophagy proteins can function as proviral factors required for HCV replication (14). Autophagy degrades macromolecules and organelles. Based on the means by which cargo is delivered to the lysosomes, three different autophagy pathways are described: macroautophagy, microautophagy, and chaperone-mediated autophagy (CMA). At first, autophagy was considered a nonselective bulk degradation process. CMA, however, results in specific degradation of the cytosolic proteins in a molecule-by-molecule fashion. Most known substrates for CMA contain a peptide sequence biochemically related to KFERQ (12). Although the typical KFERQ peptide motif is not found in HNF-1α protein, it is possible that KFERQ-like sequences can be generated by post-translational modifications. It is also possible that HNF-1α protein possesses other degradation motifs. The molecular mechanism underlying NS5A-dependent lysosomal degradation of HNF-1α protein needs to be elucidated.

HNF-1α is a homeodomain-containing transcription factor, which is expressed in the liver, pancreatic β cells, and other tissues (1). Intriguingly, HNF-1α is known to play a crucial role in diabetes. Heterozygous germ line mutations in the gene encoding HNF-1α are responsible for an autosomal dominant form of non-insulin-dependent diabetes, MODY3 (40). Mutations in the HNF-1α gene disrupt GLUT2 function as a glucose sensor in pancreatic β cells, resulting in severe insulin secretory defects (39). It is unclear whether HNF-1α mutations in the liver affect glucose homeostasis in MODY3 patients. Two strains of HNF-1α-deficient mice have been reported. The mice of the first strain, created using standard methods for making knockout mice, are born normally, but most die postnatally around the weaning period after a progressive wasting syndrome (31). Mice of the second strain, created using the Cre-loxP recombination method, had a normal life span (20). The knockout mice of the second strain were dwarfed, diabetic, and infertile. Moreover, the knockout mice had enlarged livers and exhibited progressive liver damage.

HNF-1α was also identified as a tumor suppressor gene involved in human liver tumorigenesis since biallelic inactivating mutations of the HNF-1α gene were found in 50% of hepatocellular adenomas and, in rare cases, of well-differentiated hepatocellular carcinomas developed in the absence of cirrhosis (5).

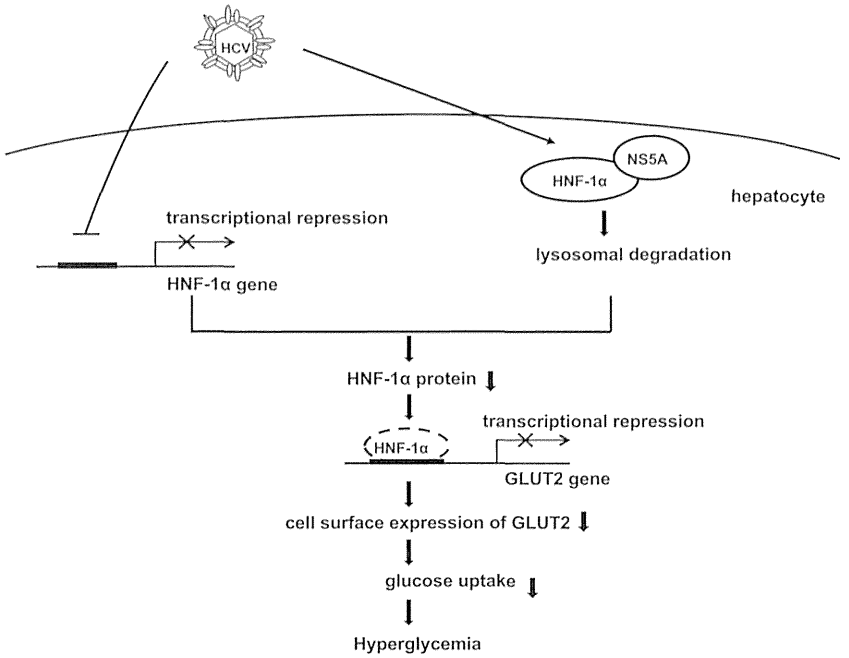

FIG 8 A proposed mechanism of the HCV-induced suppression of GLUT2 via downregulation of HNF-1α. HCV infection downregulates HNF-1α at transcriptional and posttranslational levels, resulting in suppression of GLUT2 gene transcription. HCV NS5A protein physically interacts with HNF-1α protein and enhances lysosomal degradation of HNF-1α protein.

Moreover, HNF-1α has been shown to regulate a large number of genes related to glucose, fatty acid, bile acid, cholesterol, and lipoprotein metabolisms as well as inflammation (1). Therefore, it is possible that HCV-induced downregulation of HNF-1α may play a crucial role in metabolic disorders as well as tumorigenesis.

To determine which HCV protein is involved in the suppression of the GLUT2 promoter, we examined the effects of transient expression of HCV proteins on GLUT2 promoter activity. Overexpression of NS5A suppressed GLUT2 promoter activity, whereas overexpression of p7 enhanced GLUT2 promoter activity (Fig. 5A). SGR cells express NS5A protein but lack p7 protein. FGR cells express both NS5A protein and p7 protein. However, GLUT2 promoter activity was suppressed in both SGR and FGR cells (Fig. 2B). This discrepancy between transient expression system and replicon cells may result from the differences in trafficking of p7 because it is a complex process potentially regulated by both the cleavage from its upstream signal peptides and targeting signals within the protein sequence (15).

We previously reported that HCV infection promotes hepatic gluconeogenesis in HCV J6/JFH1-infected Huh-7.5 cells (11). HCV infection transcriptionally upregulates the genes for phosphoenolpyruvate carboxykinase (PEPCK) and glucose 6-phosphatase (G6Pase), the rate-limiting enzymes for hepatic gluconeogenesis. We demonstrated that gene expression of PEPCK and G6Pase was regulated by the transcription factor forkhead box O1 (FoxO1) in HCV-infected cells. Phosphorylation of the FoxO1 at Ser319 was markedly diminished in HCV-infected cells, resulting in increased nuclear accumulation of FoxO1. HCV NS5A protein was directly linked with FoxO1-dependent increased gluconeogenesis. HCV-induced downregulation of GLUT2 expression and upregulation of gluconeogenesis may cooperatively contribute to development of type 2 diabetes in HCV-infected patients at least to some extent. HCV-induced downregulation of GLUT2 expression and upregulation of gluconeogenesis may result in high concentrations of glucose in HCV-infected hepatocytes. As suggested in a recent study, low glucose concentrations in the hepatocytes inhibit HCV replication (28). Therefore, high glucose levels in the hepatocytes may confer an advantage in efficient replication of HCV.

In conclusion, we provided evidence suggesting that HCV infection downregulates HNF-1α expression at both transcriptional and posttranslational levels. HCV-induced downregulation of HNF-1α may play a crucial role in glucose metabolic disorders caused by HCV infection. Strategies aimed at HCV-induced downregulation of HNF-1α protein may lead to the development of new therapeutic agents for HCV-induced diabetes.

ACKNOWLEDGMENTS

We are grateful to C. M. Rice (Rockefeller University, New York, NY) for providing Huh-7.5 cells and pFL-J6/JFH1, R. Bartenschlager (University of Heidelberg, Heidelberg, Germany) for providing an HCV subgenomic RNA replicon (pFK5B/2884Gly), and N. Kato (Okayama University, Okayama, Japan) for providing an HCV full-genome RNA replicon (pON/C-5B). We thank T. Adachi, M. Makimoto, K. Tsubaki, Y. Yasui, A. Asahi, M. Kohmoto, and Y.-H. Ide for their technical assistance. We also thank K. Hachida for secretarial work.

This work was supported in part by grants-in-aid for research on hepatitis from the Ministry of Health, Labor, and Welfare, Japan, and the Ministry of Education, Culture, Sports, Science, and Technology (MEXT), Japan. This work was also supported in part by the Japan Initiative for Global Research Network on Infectious Diseases program of MEXT, Japan. This study was also carried out as part of the Global Center of Excellence program of the Kobe University Graduate School of Medicine and the Science and Technology Research Partnership for Sustain-

able Development program of the Japan Science and Technology Agency and the Japan International Cooperation Agency.

We have no potential conflicts of interest to report.

REFERENCES

1. **Armendariz AD, Krauss RM.** 2009. Hepatic nuclear factor 1-alpha: inflammation, genetics, and atherosclerosis. Curr. Opin. Lipidol. **20**:106–111.
2. **Ban N, et al.** 2002. Hepatocyte nuclear factor-1α recruits the transcriptional co-activator p300 on the GLUT2 gene promoter. Diabetes **51**:1409–1418.
3. **Blight KJ, Kolykhalov AA, Rice CM.** 2000. Efficient initiation of HCV RNA replication in cell culture. Science **290**:1972–1974.
4. **Blight KJ, McKeating JA, Rice CM.** 2002. Highly permissive cell lines for subgenomic and genomic hepatitis C virus RNA replication. J. Virol. **76**: 13001–13014.
5. **Bluteau O, et al.** 2002. Bi-allelic inactivation of TCF1 in hepatic adenomas. Nat. Genet. **32**:312–315.
6. **Bungyoku Y, et al.** 2009. Efficient production of infectious hepatitis C virus with adaptive mutations in cultured hepatoma cells. J. Gen. Virol. **90**:1681–1691.
7. **Cha JY, Kim H, Kim KS, Hur MW, Ahn Y.** 2000. Identification of transacting factors responsible for the tissue-specific expression of human glucose transporter type 2 isoform gene. Cooperative role of hepatocyte nuclear factors 1α and 3β. J. Biol. Chem. **275**:18358–18365.
8. **Denamur S, et al.** 2011. Role of oxidative stress in lysosomal membrane permeabilization and apoptosis induced by gentamicin, an aminoglycoside antibiotic. Free Radic. Biol. Med. **51**:1656–1665.
9. **Deng L, et al.** 2008. Hepatitis C virus infection induces apoptosis through a Bax-triggered, mitochondrion-mediated, caspase 3-dependent pathway. J. Virol. **82**:10375–10385.
10. **Deng L, et al.** 2006. NS3 protein of Hepatitis C virus associates with the tumour suppressor p53 and inhibits its function in an NS3 sequence-dependent manner. J. Gen. Virol. **87**:1703–1713.
11. **Deng L, et al.** 2011. Hepatitis C virus infection promotes hepatic gluconeogenesis through an NS5A-mediated, FoxO1-dependent pathway. J. Virol. **85**:8556–8568.
12. **Dice JF.** 2007. Chaperone-mediated autophagy. Autophagy **3**:295–299.
13. **Dionisio N, et al.** 2009. Hepatitis C virus NS5A and core proteins induce oxidative stress-mediated calcium signalling alterations in hepatocytes. J. Hepatol. **50**:872–882.
14. **Dreux M, Chisari FV.** 2011. Impact of the autophagy machinery on hepatitis C virus infection. Viruses **3**:1342–1357.
15. **Griffin S, Clarke D, McCormick C, Rowlands D, Harris M.** 2005. Signal peptide cleavage and internal targeting signals direct the hepatitis C virus p7 protein to distinct intracellular membranes. J. Virol. **79**:15525–15536.
16. **He Y, Staschke KA, Tan SL.** 2006. HCV NS5A: a multifunctional regulator of cellular pathways and virus replication. *In* Tan SL (ed), Hepatitis C viruses: genomes and molecular biology. Horizon Bioscience, Norfolk, United Kingdom. http://www.ncbi.nlm.nih.gov/books/NBK1621/.
17. **Ikeda M, et al.** 2005. Efficient replication of a full-length hepatitis C virus genome, strain O, in cell culture, and development of a luciferase reporter system. Biochem. Biophys. Res. Commun. **329**:1350–1359.
18. **Inubushi S, et al.** 2008. Hepatitis C virus NS5A protein interacts with and negatively regulates the non-receptor protein tyrosine kinase Syk. J. Gen. Virol. **89**:1231–1242.
19. **Kasai D, et al.** 2009. HCV replication suppresses cellular glucose uptake through down-regulation of cell surface expression of glucose transporters. J. Hepatol. **50**:883–894.
20. **Lee YH, Sauer B, Gonzalez FJ.** 1998. Laron dwarfism and non-insulin-dependent diabetes mellitus in the Hnf-1α knockout mouse. Mol. Cell Biol. **18**:3059–3068.
21. **Lemon SM, Walker C, Alter MJ, Yi M.** 2007. Hepatitis C virus, p 1291–1304. *In* Knipe DM, et al (ed), Fields virology, 5th ed. Lippincott Williams & Wilkins, Philadelphia, PA.
22. **Li ZY, Yang Y, Ming M, Liu B.** 2011. Mitochondrial ROS generation for regulation of autophagic pathways in cancer. Biochem. Biophys. Res. Commun. **414**:5–8.
23. **Lindenbach BD, et al.** 2005. Complete replication of hepatitis C virus in cell culture. Science **309**:623–626.
24. **Macheda ML, Rogers S, Best JD.** 2005. Molecular and cellular regulation of glucose transporter (GLUT) proteins in cancer. J. Cell Physiol. **202**: 654–662.
25. **Malecki MT, Mlynarski W.** 2008. Monogenic diabetes: implications for therapy of rare types of disease. Diabetes Obes. Metab. **10**:607–616.
26. **Mason AL, et al.** 1999. Association of diabetes mellitus and chronic hepatitis C virus infection. Hepatology **29**:328–333.
27. **Murakami K, et al.** 2006. Production of infectious hepatitis C virus particles in three-dimensional cultures of the cell line carrying the genome-length dicistronic viral RNA of genotype 1b. Virology **351**:381–392.
28. **Nakashima K, Takeuchi K, Chihara K, Hotta H, Sada K.** 2011. Inhibition of hepatitis C virus replication through adenosine monophosphate-activated protein kinase-dependent and -independent pathways. Microbiol. Immunol. **55**:774–782.
29. **Negro F.** 2011. Mechanisms of hepatitis C virus-related insulin resistance. Clin. Res. Hepatol Gastroenterol. **35**:358–363.
30. **Negro F, Alaei M.** 2009. Hepatitis C virus and type 2 diabetes. World J. Gastroenterol. **15**:1537–1547.
31. **Pontoglio M, et al.** 1996. Hepatocyte nuclear factor 1 inactivation results in hepatic dysfunction, phenylketonuria, and renal Fanconi syndrome. Cell **84**:575–585.
32. **Qadri I, et al.** 2004. Induced oxidative stress and activated expression of manganese superoxide dismutase during hepatitis C virus replication: role of JNK, p38 MAPK and AP-1. Biochem. J. **378**:919–928.
33. **Shirakura M, et al.** 2007. E6AP ubiquitin ligase mediates ubiquitylation and degradation of hepatitis C virus core protein. J. Virol. **81**:1174–1185.
34. **Takeda J, Kayano T, Fukomoto H, Bell GI.** 1993. Organization of the human GLUT2 (pancreatic beta-cell and hepatocyte) glucose transporter gene. Diabetes **42**:773–777.
35. **Tellinghuisen TL, Marcotrigiano J, Gorbalenya AE, Rice CM.** 2004. The NS5A protein of hepatitis C virus is a zinc metalloprotein. J. Biol. Chem. **279**:48576–48587.
36. **Tellinghuisen TL, Marcotrigiano J, Rice CM.** 2005. Structure of the zinc-binding domain of an essential component of the hepatitis C virus replicase. Nature **435**:374–379.
37. **Wakita T, et al.** 2005. Production of infectious hepatitis C virus in tissue culture from a cloned viral genome. Nat. Med. **11**:791–796.
38. **Wang AG, et al.** 2009. Non-structural 5A protein of hepatitis C virus induces a range of liver pathology in transgenic mice. J. Pathol. **219**:253–262.
39. **Wang H, Maechler P, Hagenfeldt KA, Wollheim CB.** 1998. Dominant-negative suppression of HNF-1alpha function results in defective insulin gene transcription and impaired metabolism-secretion coupling in a pancreatic beta-cell line. EMBO J. **17**:6701–6713.
40. **Yamagata K, et al.** 1996. Mutations in the hepatocyte nuclear factor-1α gene in maturity-onset diabetes of the young (MODY3). Nature **384**:455–458.

Toxicology and Applied Pharmacology 282 (2015) 237–243

Contents lists available at ScienceDirect

Toxicology and Applied Pharmacology

journal homepage: www.elsevier.com/locate/ytaap

Mitochondrial iron accumulation exacerbates hepatic toxicity caused by hepatitis C virus core protein

Shuichi Sekine [a], Konomi Ito [a], Haruna Watanabe [a], Takafumi Nakano [a], Kyoji Moriya [b], Yoshizumi Shintani [b], Hajime Fujie [b], Takeya Tsutsumi [b], Hideyuki Miyoshi [b], Hidetake Fujinaga [b], Seiko Shinzawa [b], Kazuhiko Koike [b], Toshiharu Horie [a,*]

[a] Laboratory of Biopharmaceutics, Graduate School of Pharmaceutical Sciences, Chiba University, 1-8-1 Inohana, Chuo-ku, Chiba 260-8675, Japan
[b] Department of Internal Medicine, Graduate School of Medicine, The University of Tokyo, 7-3-1 Hongo, Bunkyo-ku, Tokyo 113-8655, Japan

ARTICLE INFO

Article history:
Received 8 September 2014
Revised 9 December 2014
Accepted 16 December 2014
Available online 27 December 2014

Keywords:
Ca^{2+} uniporter
Fenton reaction
Reactive oxygen species
Ru360
Hepatitis C virus

ABSTRACT

Patients with long-lasting hepatitis C virus (HCV) infection are at major risk of hepatocellular carcinoma (HCC). Iron accumulation in the livers of these patients is thought to exacerbate conditions of oxidative stress. Transgenic mice that express the HCV core protein develop HCC after the steatosis stage and produce an excess of hepatic reactive oxygen species (ROS). The overproduction of ROS in the liver is the net result of HCV core protein-induced dysfunction of the mitochondrial respiratory chain. This study examined the impact of ferric nitrilacetic acid (Fe-NTA)-mediated iron overload on mitochondrial damage and ROS production in HCV core protein-expressing HepG2 (human HCC) cells (Hep39b cells). A decrease in mitochondrial membrane potential and ROS production were observed following Fe-NTA treatment. After continuous exposure to Fe-NTA for six days, cell toxicity was observed in Hep39b cells, but not in mock (vector-transfected) HepG2 cells. Moreover, mitochondrial iron (^{59}Fe) uptake was increased in the livers of HCV core protein-expressing transgenic mice. This increase in mitochondrial iron uptake was inhibited by Ru360, a mitochondrial Ca^{2+} uniporter inhibitor. Furthermore, the Fe-NTA-induced augmentation of mitochondrial dysfunction, ROS production, and cell toxicity were also inhibited by Ru360 in Hep39b cells. Taken together, these results indicate that Ca^{2+} uniporter-mediated mitochondrial accumulation of iron exacerbates hepatocyte toxicity caused by the HCV core protein.

Introduction

Hepatitis C virus (HCV) infection is a major cause of chronic liver disease. About 120–200 million people are infected with HCV, increasing their risk of developing chronic hepatitis, cirrhosis, and eventually hepatocellular carcinoma (HCC) (Ikeda et al., 1998; Nishioka et al., 1991). The HCV genome is approximately 9.6 kb in size and encodes a polyprotein of ~3000 amino acids. The large HCV polyprotein is cleaved by host and viral proteases to generate at least ten smaller proteins, including four structural proteins (one core protein, two envelope proteins, and the E1, E2, and p7 ion channels) (Bukh et al., 1995) and six non-structural proteins (NH2-NS2, NS3, NS4A, NS4B, NS5A, and NS5B-COOH) (Bartenschlager and Lohmann, 2000). These proteins participate in viral replication and also influence cellular functions of the host.

Oxidative stress is commonly observed following HCV infection and is caused by increased levels of cellular reactive oxygen species (ROS) or by changes in cellular antioxidant capacities (Choi and Ou, 2006; Oberley, 2002; Otani et al., 2005). In particular, HCV core protein is known to be closely associated with the mitochondria and causes the increase in host ROS production, lipid peroxidation (Lau et al., 1998; Moriya et al., 2001; Okuda et al., 2002) and mitochondrial Ca^{2+} uptake. HCV core protein also reduces GSH and NADPH concentrations and mitochondrial complex I activities. These undertakings ultimately disrupt mitochondrial membrane permeability and trigger mitochondrial dysfunction (Wang et al., 2010; Wang and Weinman, 2006). As mitochondrial function is the master regulator of cellular energy and apoptotic cell death, mitochondrial injury can culminate in metabolic deficits and steatohepatitis, further exacerbating cell injury and dysfunction.

Due to the relationship between chronic HCV infection and the development of HCC, numerous studies have attempted to identify the HCV proteins that are responsible for hepatocarcinogenesis. These studies indicate that the HCV core protein can promote the immortalization of primary human hepatocytes (Ray et al., 2000), whereas the non-

Abbreviations: HCV, hepatitis C virus; HCC, hepatocellular carcinoma; ROS, reactive oxygen species; Fe-NTA, ferric nitrilacetic acid; JC-1, 5,5′,6,6′-tetrachrolo-1,1′,3,3′-tetraethylbenzimidazoly-carbocyanine iodide; CCCP, carbonyl cyanide-m-chlorophenyl hydrazine; MTT, 3-(4,5-dimethylthiazol-2-yl)-2,5-diphenyltetrazolium bromide; HPF, hydroxyphenyl fluorescein; ANT, adenine nucleotide translocator; HRP, horseradish peroxidase; DMEM, Dulbecco's Modified Eagle's Medium; CL, chemiluminescence; TTBS, Tris-buffered saline/0.05% Tween 20; BSA, bovine serum albumin; Hep39b, HCV core protein-expressing HepG2; Hepswx, vector-transfected HepG2.

* Corresponding author at: Faculty of Pharmaceutical Sciences, Teikyo Heisei University, 4-21-2 Nakano, Nakano-ku, Tokyo 164-8530, Japan. Fax: +81 3 5860 4237.
E-mail address: t.horie@thu.ac.jp (T. Horie).

http://dx.doi.org/10.1016/j.taap.2014.12.004
0041-008X/

structural proteins NS3 and NS4B can transform NIH 3T3 cells, either individually or in combination with Ha-ras (Park et al., 2000). Iron overload in the liver, which is associated with the genetic disorder hereditary hemochromatosis, has been thought to increase the risk of HCC by about 200-fold (Bonkovsky et al., 1997; Kowdley, 2004). For example, the livers of patients afflicted with HCV are characterized by the elevated expression of transferrin receptor 1 and hepcidin, both of which stimulate iron uptake into hepatocytes (Bonkovsky et al., 1997; Hayashi et al., 1994). In contrast, iron depletion (in the form of dietary iron restriction and/or phlebotomy) can improve hepatic inflammation and lower serum aminotransferase activity in HCV patients (Hayashi et al., 1994). Thus, a major precipitating factor for the pathogenesis of HCV-related liver disease has been attributed to the augmentation of oxidative stress following iron accumulation. However, no underlying cellular mechanism has yet been elucidated.

This study investigated the effect of iron exposure on mitochondrial dysfunction, ROS production and cell toxicity in human hepatoma cells stably expressing the HCV core protein (Hep39b cells). The underlying mechanism responsible for mitochondrial iron accumulation in Hep39b cells and in the livers of HCV core protein-expressing transgenic mice was also examined.

Materials and methods

Chemicals and reagents. Ferric nitrate nonahydrate, nitrilotriacetic acid (NTA), 5,5′,6,6′-tetrachrolo-1,1′,3,3′-tetraethylbenzimidazolycarbocyanine iodide (JC-1), carbonyl cyanide-m-chlorophenyl hydrazine (CCCP) and G418 disulfate were from Sigma Aldrich (St. Louis, MO). MitoTracker® Red was from Invitrogen (Carlsbad, CA). $^{59}FeSO_4$ was from Perkin-Elmer (Waltham, MA). Ru360 was from Merck Millipore Japan (Tokyo, Japan). MTT [3-(4,5-dimethylthiazol-2-yl)-2,5-diphenyltetrazolium bromide] was from Wako Pure Chemical Industries, Ltd. (Osaka, Japan). Hydroxyphenyl fluorescein (HPF) was from Sekisui Medical Co., Ltd. (Tokyo, Japan). Adenine nucleotide translocator (ANT) goat polyclonal IgG, CCDC109A goat polyclonal IgG and horseradish peroxidase (HRP)-conjugated anti-goat IgG were from Santa Cruz Biotechnology, Inc. (Santa Cruz, CA). All chemicals and solvents were of analytical grade.

Preparation of Fe-NTA. The Fe-NTA complex was prepared as described by Awai et al. (1979). Briefly, ferric nitrate was dissolved in 1 N HCl to form a 50 mM solution, and NTA was dissolved in 1 N NaOH to form a 150 mM solution. Equal volumes of the two solutions were mixed just before the experiment, and the pH was adjusted to 7.4 with $NaHCO_3$.

Assessment of cytotoxicity. Cytotoxicity was assessed by the MTT assay. Briefly, Hep39b and Hepswx cells were seeded into 96 well culture plates at a density of 8.4×10^3 cells/well and were exposed to various concentrations of Fe-NTA the following day, the medium was replaced with fresh medium containing the same component every 24 h. In some conditions, cells were treated with 20 μM Ru360, a mitochondrial Ca^{2+} uniporter inhibitor, for 1 h prior to Fe-NTA exposure. After six days, the cell culture medium was replaced by 50 μl MTT solution (5 mg/ml MTT in phenol red-free Dulbecco's Modified Eagle's Medium (DMEM)), and the cells were incubated for 2 h at 37 °C. To dissolve the reduced MTT crystals, 200 μl isopropanol was added. The absorbance of the dye was measured at a wavelength of 570 nm, and the turbidity of the cells (background absorbance) was measured at a reference wavelength of 630 nm. The absorbance of the controls (Hepswx and Hep39b) was set at 100%, and cytotoxicity was calculated as the absorbance of the experimental sample relative to that of the control.

Assessment of ROS production. ROS production was first assessed by chemiluminescence (CL) analysis. Briefly, cells were seeded into 35 mm glass-bottomed dishes at a density of 2.5×10^5 cells/dish and exposed to 300 μM Fe-NTA the following day, the medium was replaced with fresh medium containing the same component every 24 h. In some cases, cells were treated with Ru360 for 1 h prior to Fe-NTA treatment. After five days, the cell culture medium was replaced with phenol red-free DMEM containing Fe-NTA and Ru360, and the dish was protected from light. The following day, spontaneous CL was measured using a single photoelectron counting system (CLD-10; Tohoku Electronic Industrial Co., Ltd., Sendai, Japan), as described previously (Maeda et al., 2010). Emission was expressed in counts/10 min/mg protein.

ROS production was also assessed using HPF as a fluorescent probe for the selective detection of hydroxyl radicals. Briefly, cells were seeded into 35 mm glass-bottomed dishes, as described for CL analysis. After 7 days, the cell culture medium was replaced with modified Hanks' balanced salt solution (HBSS) containing 10 mM HEPES, 1 mM $MgCl_2$, 2 mM $CaCl_2$ and 2.7 mM glucose (pH 7.4). Next, 10 μM HPF and 20 nM MitoTracker® Red (a fluorescent probe for the mitochondria) were added, and cells were incubated for 15 min at 37 °C. Images of HPF and MitoTracker® Red staining were obtained using a laser scanning confocal microscope (FV300; Olympus Optical Co., Ltd., Tokyo, Japan). The wavelengths (excitation/emission) for the detection of HPF (green) and MitoTracker® Red (red) were 488 nm/515 nm and 579 nm/599 nm, respectively.

Assessment of mitochondrial membrane potential. Measurement of mitochondrial membrane potential was performed using the JC-1 stain, a lipophilic cation fluorescent dye that accumulates in the mitochondria. At a low mitochondrial membrane potential, the JC-1 dye exists as a monomeric molecule and fluoresces green, whereas at a higher membrane potential the JC-1 dye forms polymeric aggregates and fluoresces red. A fall in the mitochondrial membrane potential is therefore indicated by a decrease in the ratio of red signal to green signal.

Cells were cultured in 96 well black culture plates at a density of 8.4×10^3 cells/well and exposed to various concentrations of Fe-NTA the following day, the medium was replaced with fresh medium containing the same component every 24 h. After six days, the culture medium was replaced with 200 μl JC-1 solution (10 μg/ml JC-1 in HBSS), and cells were incubated in the dark for 30 min at 37 °C. After washing twice with HBSS, the absorbance of the cells in each well was immediately measured using a fluorescence plate reader with the excitation and emission wavelengths set at 490 nm and 530 nm (green)/590 nm (red), respectively.

Animals. The production of transgenic mice expressing the HCV core protein has been described previously (Moriya et al., 2001). Briefly, the HCV core protein gene was placed downstream of a transcriptional regulatory region from the hepatitis B virus and introduced into C57BL/6 mouse embryos (Clea Japan, Tokyo, Japan). All of the animals were treated humanely in accordance with the guidelines issued by the National Institute of Health and all procedures described below were approved by the animal care committee of Chiba University.

Isolation of mouse liver mitochondria. The mouse liver mitochondrial fraction was prepared according to a previously described method (Masubuchi et al., 2002). Livers were isolated from two mice and placed in ice-cold buffer containing 250 mM sucrose, 10 mM HEPES–KOH, and 0.5 mM EGTA (pH 7.4). Livers were cut into small cubes with scissors in the same buffer and homogenized five times with a Potter homogenizer. The homogenates were diluted to 0.25 g liver/ml and were centrifuged at 770 ×*g* for 5 min at 4 °C. The resulting supernatant was decanted and further centrifuged at 9800 ×*g* for 10 min. The pellet was resuspended to yield a concentration of 0.5 g liver/ml in buffer containing 250 mM sucrose, 10 mM HEPES–KOH and 0.3 mM EGTA (pH 7.4), and centrifuged at 4500 ×*g* for 10 min. The pellet was resuspended to yield a concentration of 1 g liver/ml in the same buffer and centrifuged at 2000 ×*g* for 2 min, followed by further centrifugation at 4500 ×*g* for 8 min. The

final pellet was then resuspended in buffer containing 250 mM sucrose and 10 mM HEPES–KOH (pH 7.4) and used for further experiments.

Mitochondrial iron uptake. All experiments were conducted in a 30 °C water bath. After pre-incubation of the mitochondria in buffer containing 225 mM sucrose, 10 mM KCl, 5 mM $MgCl_2$, 5 mM KH_2PO_4, and 20 mM Tris–HCl (pH 7.4) for 1 min, Ru360 was added at a final concentration of 10 μM, $^{59}FeSO_4$ was added after 1 min, and the ^{59}Fe remaining in the mitochondria after 10 min was measured using a gamma counter.

Western blotting analysis. The mouse liver mitochondrial fraction (10 μg protein) was subjected to electrophoresis on a 12.5% polyacrylamide slab gel containing 0.1% sodium dodecyl sulfate and transferred onto an Immobilon-P Transfer Membrane filter (Millipore Corporation, Billerica, MA). The membrane was blocked for 1 h at room temperature with Tris-buffered saline/0.05% Tween 20 (TTBS) containing 3% bovine serum albumin (BSA) and probed overnight at 4 °C with the CCDC109A goat polyclonal IgG (1:200) against the Ca^{2+} uniporter and the ANT goat polyclonal IgG (1:1000). The membrane was then incubated for 1 h at room temperature with donkey anti-goat IgG-HRP (1:3333). All antibodies were diluted in TTBS containing 0.1% BSA. Immunoreactive bands were detected using a LAS-1000 imaging system (Fuji Film, Tokyo, Japan) and an enhanced CL system (GE Healthcare, Little Chalfont, Buckinghamshire, UK).

Statistical analysis. All data are represented as the mean ± the standard error (S.E.). Data were statistically analyzed by using one-way ANOVA followed by the Bonferroni test for multiple comparison. For comparison among two groups, two-tailed Student's t-test was adopted. Differences between means at the level of $P < 0.05$ were considered significant.

Results

Iron-induced cytotoxicity in HCV core protein-expressing HepG2 cells

The iron uptake system is perturbed in HCV-infected hepatocytes due to elevated expression of transferrin receptor 1. However, because of its hydrophobicity, Fe-NTA is taken up into the cell in a transferrin receptor 1-independent manner by passive diffusion. Fe-NTA is then converted into free Fe^{2+} by several types of esterases. Therefore, Fe-NTA was used in the current study to control for intrinsic differences in active iron uptake between HCV core protein-expressing HepG2 cells (Hep39b cells) and vector-transfected HepG2 cells (Hepswx cells). After treatment with Fe-NTA for six days, cytotoxicity was assessed using the MTT assay. Concentration-dependent cytotoxicity of Fe-NTA against Hep39b cells was observed. By contrast, no cytotoxicity was observed against control Hepswx cells at Fe-NTA concentrations of less than 1000 μM (Fig. 1). These data indicate that HCV core protein expression affects the susceptibility of hepatocytes to Fe-NTA-induced iron cytotoxicity.

Effect of iron accumulation on ROS production in HCV core protein-expressing versus control hepatocytes

To directly measure free radical formation, we took advantage of methodology for measuring spontaneous CL and compared the levels of CL in HCV core protein-expressing Hep39b and control Hepswx cells (Fig. 2a). As shown in Fig. 2a, spontaneous CL was significantly higher in Hep39b cells by approximately 156% compared with that in Hepswx cells (6015 versus 3856 arbitrary units; $P < 0.01$). In the presence of 300 μM Fe-NTA, iron-induced CL was also significantly higher in Hep39b cells relative to Hepswx cells (2.61-fold versus 1.54-fold increase; $P < 0.01$ and $P < 0.001$, respectively) (Fig. 2a).

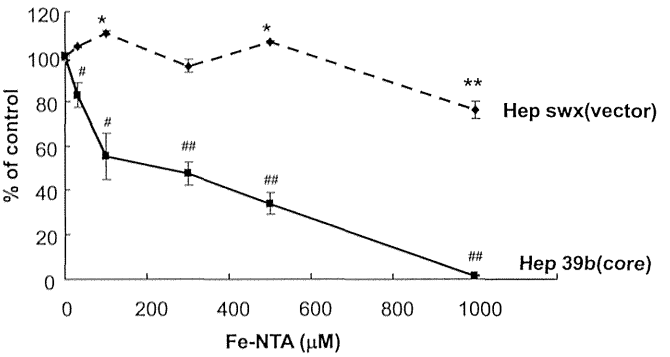

Fig. 1. Iron-induced cytotoxicity in control versus HCV core protein-expressing hepatocytes. Hepswx (dashed line) and Hep39b (solid line) cells were exposed with Fe-NTA (30, 100, 300, 500 and 1000 μM) for six days. Hepatotoxicity was determined using the MTT assay. Viability was calculated as the absorbance of the experimental sample relative to that of the controls (without Fe-NTA treatments). Values are the mean ± the S.E. $^{*}P < 0.05$ and $^{**}P < 0.01$, significantly different from the control (without Fe-NTA). $^{\#}P < 0.05$ and $^{\#\#}P < 0.01$, significantly different from respective control cells (Hepswx) ($n = 6$).

Effect of iron accumulation on mitochondrial ROS production

Mitochondria are a major source of ROS production. Therefore, we next examined the production of mitochondrial hydroxyl radicals by free iron catalyzation (i.e., the Fenton reaction). Since increased production of ROS was observed in Hep39b cells in the presence of Fe-NTA, we next examined mitochondrial ROS production by double staining with MitoTracker® Red (red), a fluorescent probe for the mitochondria, and HPF (green), a fluorescent probe for the selective detection of hydroxyl radicals. As shown in Fig. 2b, a strong fluorescent signal derived from HPF was observed in Hep39b cells in the presence of Fe-NTA. This fluorescence overlapped with that generated by MitoTracker® Red (Fig. 2b). The fluorescent signal derived from HPF in overlapped area was significantly higher in Hep39b cells by approximately 200% compared with that in Hepswx cells (Fig. 2c). These data indicate that mitochondrial hydroxyl radical production was increased in the presence of the HCV core protein and Fe-NTA.

Effect of HCV core protein on mitochondrial membrane potential

The HCV core protein is known to inhibit mitochondrial respiratory complex I activity (Korenaga et al., 2005). Inhibition of complex I leads to ROS formation due to premature electron leakage from the complex. Therefore, we next examined the effect of Fe-NTA on mitochondrial membrane potential in Hep39b cells by using JC-1, a lipophilic cationic dye that selectively enters the mitochondria and reversibly changes color from green to red as the membrane potential increases. Fig. 3 demonstrates that the mitochondrial membrane potential was decreased in HCV core protein-expressing Hep39b cells compared with control Hepswx cells. The decrease in membrane potential was significantly increased following exposure to Fe-NTA (300 and 1000 μM) for six days (Fig. 3).

Mitochondrial free iron uptake in HCV core protein-expressing versus control hepatocytes

Because mitochondrial hydroxyl radical production was increased in the presence of Fe-NTA (Fig. 2), the uptake of free iron into isolated mitochondria was next examined. To ensure a sufficient quantity and quality of the mitochondria for this experiment, mitochondria were isolated from the liver of HCV core protein-expressing transgenic and wild-type (control) mice. Fig. 4 shows that the concentration of mitochondrial free

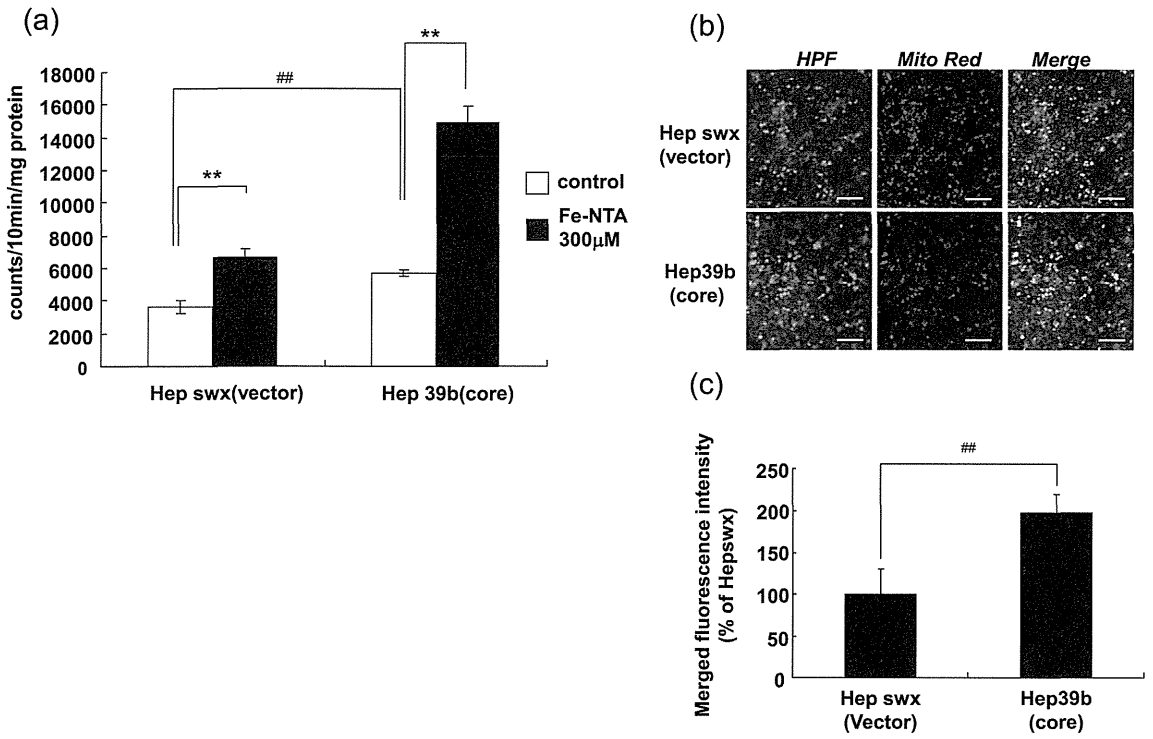

Fig. 2. Iron-induced mitochondrial ROS production is enhanced in HCV core protein-expressing hepatocytes. (a) Hepswx and Hep39b cells were exposed to Fe-NTA (300 μM) for six days. ROS production was determined using a CL analyzer. Detected counts were normalized by protein content of cell lysate. Values are given as the mean ± the S.E. $^{**}P < 0.01$ and $^{\#\#}P < 0.01$, significantly different from respective control (n = 3–4). (b) Hepswx and Hep39b cells were pretreated with HPF (green) and MitoTracker® Red (red). Mitochondrial ROS production was determined by the strength of yellow fluorescence in the merged pictures. The scale bar represents 100 μm. (c) Analysis of merged fluorescence microscopy images was done by ImageJ. Integrated density of merged area was automatically selected and fluorescence intensity of HPF was calculated within the merged area of 200–300 cells.

iron ($^{59}Fe^{2+}$) was significantly increased in the mitochondria derived from the transgenic versus the control mouse liver (62.2 ± 4.2 versus 79.5 ± 2.1 pmol/mg protein, respectively; $P < 0.05$), whereas the passive diffusion of $^{59}Fe^{2+}$ into the mitochondria (estimated by $^{59}Fe^{2+}$ uptake at 4 °C) was 31.1 ± 3.2 pmol/10 min/mg protein in Hepswx cells, and 29.2 ± 1.8 pmol/10 min/mg protein in Hep39b cells (not significantly different). Moreover, $^{59}Fe^{2+}$ uptake into the transgenic and control mitochondria was attenuated to the same level by Ru360 (48.2 ± 4.1 versus 47.5 ± 1.2 pmol/mg protein, respectively) (Fig. 4). These data indicate that calcium uniporter plays a role in free iron uptake into the mitochondria and that the activity of the Ca^{2+} uniporter is increased by the HCV core protein.

Effect of Ru360 on Fe-NTA-induced ROS production and cytotoxicity

We next examined the effect of Ru360 on Fe-NTA-induced ROS production and cytotoxicity in Hep39b versus Hepswx cells. As shown in Fig. 5a, in the absence of Fe-NTA, Ru360 had no effect on ROS production

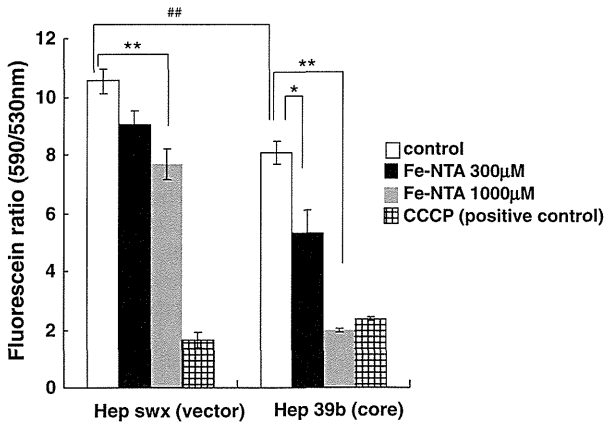

Fig. 3. The iron-induced reduction in mitochondrial membrane potential is increased by the expression of HCV core protein. Hepswx and Hep39b cells were exposed to Fe-NTA for six days. Mitochondrial membrane potential was estimated fluorometrically. Values are given as the mean ± the S.E. $^{*}P < 0.05$, $^{**}P < 0.01$ and $^{\#\#}P < 0.01$, significantly different from respective control (n = 6).

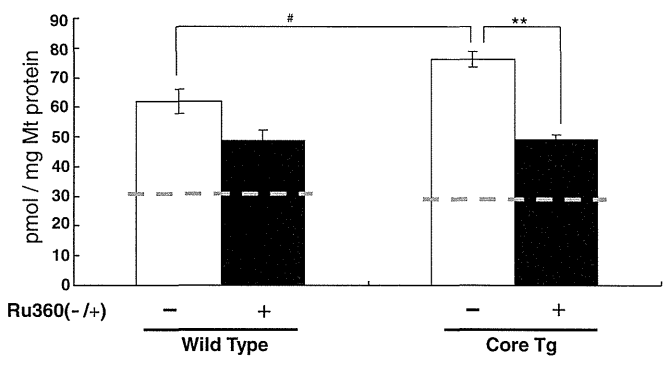

Fig. 4. Mitochondrial iron uptake is augmented by the expression of HCV core protein and inhibited by Ru360. Mitochondria were isolated from wild-type and HCV core protein transgenic (Tg) mice and exposed to $^{59}FeSO_4$ with/without Ru360. Free iron uptake was measured in the isolated mitochondria and the free iron uptake amount was normalized by mitochondrial protein content. The dashed line represents the passive diffusion into the mitochondria. Values are given as the mean ± the S.E. $^{**}P < 0.01$ and $^{\#}P < 0.05$, significantly different from respective control (n = 3–8).

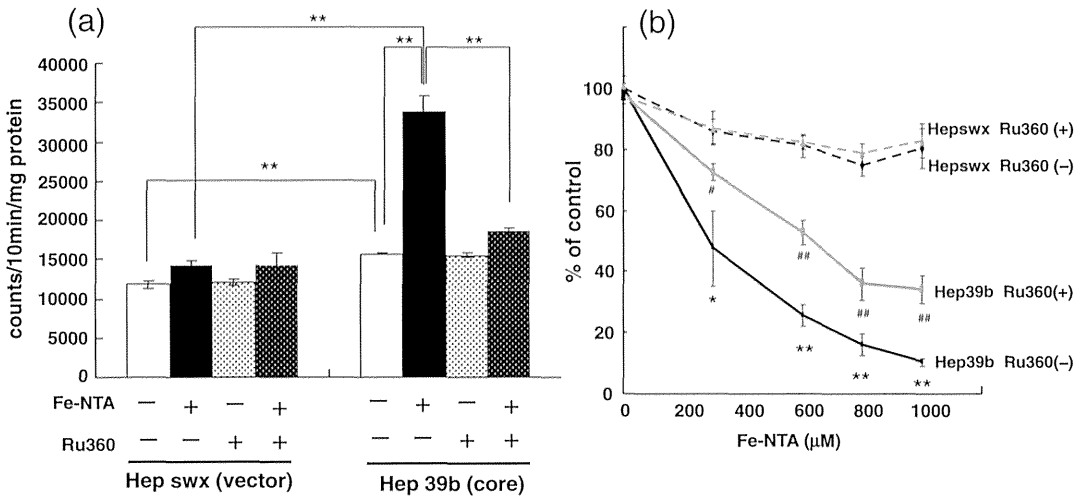

Fig. 5. Iron-induced ROS production and cytotoxicity are inhibited by Ru360 in HCV core protein-expressing hepatocytes. (a) Hepswx and Hep39b cells were exposed to Fe-NTA (300 μM) and Ru360 (20 μM) for six days. ROS production was determined using a CL analyzer. Values are given as the mean ± the S.E. $^{**}P < 0.01$, significantly different from respective control (n = 8). (b) Hepswx and Hep39b cells were exposed to Fe-NTA (300, 600, 800, and 1000 μM) and Ru360 (20 μM) for six days. Cytotoxicity was determined using the MTT assay. Values are given as the mean ± the S.E. $^{*}P < 0.05$ and $^{**}P < 0.01$, significantly different from Hepswx Ru360(−). $^{\#}P < 0.05$ and $^{\#\#}P < 0.01$, significantly different from Hep39b Ru360(−) (n = 6).

in Hepswx cells and Hep39b cells. On the other hand, Ru360 significantly suppressed Fe-NTA (300 μM)-induced ROS production in Hep39b but not Hepswx cells (Fig. 5a). Moreover, cytotoxicity following exposure to (300, 600, 800 and 1000 μM) Fe-NTA for six days was also specifically inhibited by Ru360 treatment in Hep39b cells (Fig. 5b).

Expression of the Ca^{2+} uniporter in isolated mitochondria

Given that mitochondrial free iron uptake is enhanced in HCV core protein-expressing Hep39b cells (Fig. 4), we next examined the expression of the Ca^{2+} uniporter in the mitochondria isolated from the liver of HCV core protein-expressing transgenic mice relative to control mice. As shown in Fig. 6, mitochondrial expression of the uniporter was similar in transgenic versus control mice, as assessed by Western blot analysis.

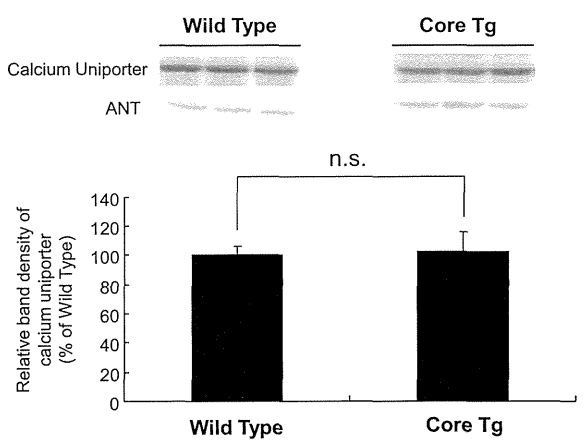

Fig. 6. Expression of mitochondrial Ca^{2+} uniporter in the livers of HCV core protein-expressing transgenic versus wild-type mice. Mitochondria were isolated from the livers of wild-type (control) and HCV core protein-expressing transgenic (Tg) mice. The expression levels of the Ca^{2+} uniporter and ANT (loading control) were determined by Western blot analysis. Mitochondrial proteins (10 μg) were loaded into each lane of the gel. The band density of the uniporter was normalized to the band density of ANT. Values are given as the mean ± the S.E. n.s.: not significantly different (n = 3).

Discussion

The accumulation of iron into the liver of HCV core protein-expressing transgenic mice fed a normal diet is similar to that observed in chronic HCV patients (Farinati et al., 1995; Kato et al., 2001). On the other hand, the expression level of hepcidin, which regulates iron metabolism by inhibiting iron absorption from the intestine and the hepatic portal system, is reportedly decreased in the liver of HCV patients and full-length HCV genome-expressing transgenic mice, but not in the liver of HCV core protein-expressing transgenic mice (Moriya et al., 2010; Muckenthaler, 2008). Therefore, although the precise regulation of iron transport into the mitochondria is essential for heme biosynthesis, hemoglobin production, and Fe–S clustering, the mechanism(s) behind mitochondrial iron homeostasis is not yet fully understood.

Previous work from our group revealed elevated ROS generation in HCV core protein-expressing transgenic mice (Moriya et al., 2001). Moreover, our previous work, along with that of others (Korenaga et al., 2005), showed that the core protein interacts with the outer mitochondrial membrane and impairs the mitochondrial respiratory chain in the normal mouse liver via inhibition of complex I activity (unpublished data). Inhibition of respiratory chain complexes ultimately leads to the overproduction of ROS via electron leakage from the mitochondria. Therefore, we hypothesized that the inducible mitochondrial iron transport system exacerbates hepatic toxicity caused by the HCV core protein.

This study employed Fe-NTA to exclude intrinsic differences in iron uptake into HCV core protein-expressing Hep39b cells and vector-transfected Hepswx cells. In addition, we demonstrated that HCV core protein-induced alterations in mitochondrial ROS production and membrane potential were augmented in the presence of iron (Figs. 2 and 3). These data may indicate that iron-dependent mitochondrial dysfunction was amplified via the Fenton reaction, which produces potent reactive free radicals (i.e., hydroxyl radicals) (Fig. 7).

Iron is absolutely essential for the sustenance of all forms of life due to its unusual ability to serve as both an electron donor and acceptor. On the other hand, free iron is also potentially toxic, which is related to its ability to donate and accept electrons within the cell. Free iron catalyzes the conversion of hydrogen peroxide into free radicals, which can cause damage to the mitochondria and cellular structures. For this reason, the iron homeostasis is strictly regulated, and the impairment of iron homeostasis is related to several diseases. In patients with HCV, hepatic

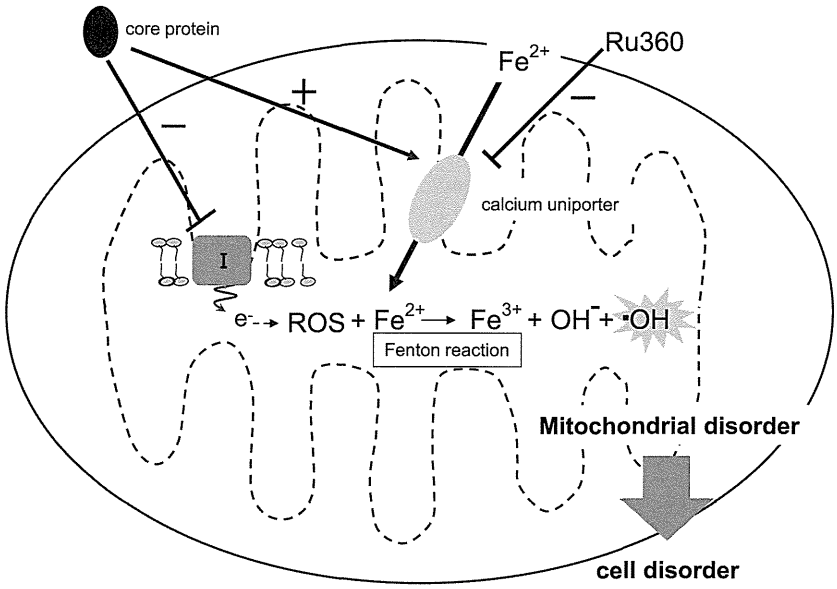

Fig. 7. Proposed mechanism of mitochondrial iron accumulation and hepatic cytotoxicity caused by the HCV core protein. The HCV core protein induces mitochondrial ROS production by inhibiting mitochondrial complex I. In addition, it is suggested that the HCV core protein stimulates mitochondrial iron uptake through the mitochondrial Ca^{2+} uniporter. The excess iron then leads to mitochondrial ROS production and mitochondrial/cellular malfunction/disorder when the HCV core protein is expressed.

and serum free iron concentrations are ~7-fold higher (12.5 mmol/g liver and 134 mg/dl, respectively) than those of a normal individual (Farinati et al., 1995; Kageyama et al., 1998; Olynyk et al., 1995; Silva et al., 2005). In this study, significant hepatotoxicity was observed at 30 μM Fe-NTA in HCV core protein-expressing Hep39b cells (Fig. 1). Therefore, a physiologically relevant concentration of iron (30 μM), which is not sufficient to induce cell toxicity by itself, was synergistic with the toxic actions of the core protein (Fig. 1). This interplay was similarly revealed by the synergy between iron and the core protein in inducing mitochondrial dysfunction and ROS production (Figs. 2 and 3).

This study further demonstrated that mitochondrial free iron uptake was partially mediated by the Ca^{2+} uniporter. The Ca^{2+} uniporter was selectively inhibited by Ru360 and exhibited an increased capacity to uptake iron into HCV core protein-expressing liver mitochondria versus normal liver mitochondria (Fig. 4). However, the expression of the uniporter was unaltered in core protein-expressing transgenic mice relative to normal mice (Fig. 6). Li et al. (2007) reported that the activity of the Ca^{2+} uniporter was up-regulated in the presence of the core protein: The in vitro incubation of mouse liver mitochondria with HCV core protein (100 ng/mg) increased the Ca^{2+} entry rate by ~2-fold. The Ca^{2+} uniporter is located in the inner mitochondrial membrane and transports not only Ca^{2+} but also other metal cationic ions (e.g., Fe^{2+}) into the mitochondrial matrix space in a mitochondrial membrane potential-dependent fashion (Bernardi, 1999).

Iron uptake was significantly suppressed to the same level by Ru360 in the mitochondria isolated from both core protein-expressing transgenic and normal mice (Fig. 4). Moreover, as free iron uptake into the mitochondria was still observed at 4 °C for both types of the mitochondria, about half of the iron (Hepswx; 31.1 ± 3.2 pmol/10 min/mg protein, Hep39b; 29.2 ± 1.8 pmol/10 min/mg protein) was estimated to enter into the mitochondria by passive diffusion (Fig. 4, dashed line). These data indicate that the up-regulation of iron uptake in the mitochondria isolated from transgenic mice was mediated by the HCV core protein-induced stimulation of Ru360-sensitive Ca^{2+} uniporter transport activity. However, the mechanism by which the core protein alters the function of the mitochondrial uniporter is still unclear, especially given that the core protein binds to the outer mitochondrial membrane, and the uniporter is located in the inner mitochondrial membrane. It is known that mitochondrial calcium uniporter possibly forms multi-molecular complex (Raffaello et al., 2012). Mitochondrial calcium uniporter function could be altered by the effect on essential regulator and/or protein involved in the assembly of the channel. In this regard, though our current study demonstrated that HCV core protein had no effect on Ca^{2+} uniporter expression (Fig. 6), it is possible that other mechanisms are involved in the HCV core protein-induced stimulation of Ca^{2+} uniporter transport activity. Further study should be addressed in the future.

Interferon-α has been used as monotherapy for chronic hepatitis C, yet only about 40–50% of hepatitis C patients experience an initial biochemical response to the cytokine. Interestingly, high iron accumulation in chronic HCV carriers is related to a poor response to interferon therapy (Walters et al., 1973). In addition, some investigators have suggested that iron removal therapy (via phlebotomy or food therapy (i.e., restriction of an iron rich-diet)) can attenuate liver damage in hepatitis C patients by still unknown mechanisms (Hayashi et al., 1994; Kato et al., 2007). The current study showed that the HCV core protein-induced mitochondrial iron uptake is responsible for exacerbating mitochondrial dysfunction and ROS production, which finally seems to lead to hepatocyte toxicity (Fig. 7). Based on these results, we suggest that inhibition of the mitochondrial Ca^{2+} uniporter may provide a new therapeutic approach to treat liver disease in HCV patients.

Conflict of interest statement

The authors declare no conflict of interest.

Acknowledgments

This work was supported by a grant-in-aid for scientific research (A) 548 (21249003) and a grant-in-aid for young scientists (B) (21790141) from the Ministry of Education, Culture, Sports, Science and Technology of Japan.

References

Awai, M., Narasaki, M., Yamanoi, Y., Seno, S., 1979. Induction of diabetes in animals by parenteral administration of ferric nitrilotriacetate. A model of experimental hemochromatosis. Am. J. Pathol. 95, 663–673.

Bartenschlager, R., Lohmann, V., 2000. Replication of hepatitis C virus. J. Gen. Virol. 81, 1631–1648.
Bernardi, P., 1999. Mitochondrial transport of cations: channels, exchangers, and permeability transition. Physiol. Rev. 79, 1127–1155.
Bonkovsky, H.L., Banner, B.F., Rothman, A.L., 1997. Iron and chronic viral hepatitis. Hepatology 25, 759–768.
Bukh, J., Miller, R.H., Purcell, R.H., 1995. Genetic heterogeneity of hepatitis C virus: quasispecies and genotypes. Semin. Liver Dis. 15, 41–63.
Choi, J., Ou, J.H., 2006. Mechanisms of liver injury. III. Oxidative stress in the pathogenesis of hepatitis C virus. Am. J. Physiol. Gastrointest. Liver Physiol. 290, G847–G851.
Farinati, F., Cardin, R., De Maria, N., Della Libera, G., Marafin, C., Lecis, E., et al., 1995. Iron storage, lipid peroxidation and glutathione turnover in chronic anti-HCV positive hepatitis. J. Hepatol. 22, 449–456.
Hayashi, H., Takikawa, T., Nishimura, N., Yano, M., Isomura, T., Sakamoto, N., 1994. Improvement of serum aminotransferase levels after phlebotomy in patients with chronic active hepatitis C and excess hepatic iron. Am. J. Gastroenterol. 89, 986–988.
Ikeda, K., Saitoh, S., Suzuki, Y., Kobayashi, M., Tsubota, A., Koida, I., et al., 1998. Disease progression and hepatocellular carcinogenesis in patients with chronic viral hepatitis: a prospective observation of 2215 patients. J. Hepatol. 28, 930–938.
Kageyama, F., Kobayashi, Y., Murohisa, G., Shimizu, E., Suzuki, F., Kikuyama, M., et al., 1998. Failure to respond to interferon-alpha 2a therapy is associated with increased hepatic iron levels in patients with chronic hepatitis C. Biol. Trace Elem. Res. 64, 185–196.
Kato, J., Kobune, M., Nakamura, T., Kuroiwa, G., Takada, K., Takimoto, R., et al., 2001. Normalization of elevated hepatic 8-hydroxy-2′-deoxyguanosine levels in chronic hepatitis C patients by phlebotomy and low iron diet. Cancer Res. 61, 8697–8702.
Kato, J., Miyanishi, K., Kobune, M., Nakamura, T., Takada, K., Takimoto, R., et al., 2007. Long-term phlebotomy with low-iron diet therapy lowers risk of development of hepatocellular carcinoma from chronic hepatitis C. J. Gastroenterol. 42, 830–836.
Korenaga, M., Wang, T., Li, Y., Showalter, L.A., Chan, T., Sun, J., et al., 2005. Hepatitis C virus core protein inhibits mitochondrial electron transport and increases reactive oxygen species (ROS) production. J. Biol. Chem. 280, 37481–37488.
Kowdley, K.V., 2004. Iron, hemochromatosis, and hepatocellular carcinoma. Gastroenterology 127, S79–S86.
Lau, J.Y., Xie, X., Lai, M.M., Wu, P.C., 1998. Apoptosis and viral hepatitis. Semin. Liver Dis. 18, 169–176.
Li, Y., Boehning, D.F., Qian, T., Popov, V.L., Weinman, S.A., 2007. Hepatitis C virus core protein increases mitochondrial ROS production by stimulation of Ca^{2+} uniporter activity. FASEB J. 21, 2474–2485.
Maeda, T., Miyazono, Y., Ito, K., Hamada, K., Sekine, S., Horie, T., 2010. Oxidative stress and enhanced paracellular permeability in the small intestine of methotrexate-treated rats. Cancer Chemother. Pharmacol. 65, 1117–1123.
Masubuchi, Y., Nakayama, S., Horie, T., 2002. Role of mitochondrial permeability transition in diclofenac-induced hepatocyte injury in rats. Hepatology 35, 544–551.
Moriya, K., Nakagawa, K., Santa, T., Shintani, Y., Fujie, H., Miyoshi, H., et al., 2001. Oxidative stress in the absence of inflammation in a mouse model for hepatitis C virus-associated hepatocarcinogenesis. Cancer Res. 61, 4365–4370.
Moriya, K., Miyoshi, H., Shinzawa, S., Tsutsumi, T., Fujie, H., Goto, K., et al., 2010. Hepatitis C virus core protein compromises iron-induced activation of antioxidants in mice and HepG2 cells. J. Med. Virol. 82, 776–792.
Muckenthaler, M.U., 2008. Fine tuning of hepcidin expression by positive and negative regulators. Cell Metab. 8, 1–3.
Nishioka, K., Watanabe, J., Furuta, S., Tanaka, E., Iino, S., Suzuki, H., et al., 1991. A high prevalence of antibody to the hepatitis C virus in patients with hepatocellular carcinoma in Japan. Cancer 67, 429–433.
Oberley, T.D., 2002. Oxidative damage and cancer. Am. J. Pathol. 160, 403–408.
Okuda, M., Li, K., Beard, M.R., Showalter, L.A., Scholle, F., Lemon, S.M., et al., 2002. Mitochondrial injury, oxidative stress, and antioxidant gene expression are induced by hepatitis C virus core protein. Gastroenterology 122, 366–375.
Olynyk, J.K., Reddy, K.R., Di Bisceglie, A.M., Jeffers, L.J., Parker, T.I., Radick, J.L., et al., 1995. Hepatic iron concentration as a predictor of response to interferon alfa therapy in chronic hepatitis C. Gastroenterology 108, 1104–1109.
Otani, K., Korenaga, M., Beard, M.R., Li, K., Qian, T., Showalter, L.A., et al., 2005. Hepatitis C virus core protein, cytochrome P450 2E1, and alcohol produce combined mitochondrial injury and cytotoxicity in hepatoma cells. Gastroenterology 128, 96–107.
Park, J.S., Yang, J.M., Min, M.K., 2000. Hepatitis C virus nonstructural protein NS4B transforms NIH3T3 cells in cooperation with the Ha-ras oncogene. Biochem. Biophys. Res. Commun. 267, 581–587.
Raffaello, A., De Stefani, D., Rizzuto, R., 2012. The mitochondrial Ca^{2+} uniporter. Cell Calcium 52, 16–21.
Ray, R.B., Meyer, K., Ray, R., 2000. Hepatitis C virus core protein promotes immortalization of primary human hepatocytes. Virology 271, 197–204.
Silva, I.S., Perez, R.M., Oliveira, P.V., Cantagalo, M.I., Dantas, E., Sisti, C., et al., 2005. Iron overload in patients with chronic hepatitis C virus infection: clinical and histological study. J. Gastroenterol. Hepatol. 20, 243–248.
Walters, G.O., Miller, F.M., Worwood, M., 1973. Serum ferritin concentration and iron stores in normal subjects. J. Clin. Pathol. 26, 770–772.
Wang, T., Weinman, S.A., 2006. Causes and consequences of mitochondrial reactive oxygen species generation in hepatitis C. J. Gastroenterol. Hepatol. 21 (Suppl. 3), S34–S37.
Wang, T., Campbell, R.V., Yi, M.K., Lemon, S.M., Weinman, S.A., 2010. Role of hepatitis C virus core protein in viral-induced mitochondrial dysfunction. J. Viral Hepat. 17, 784–793.

Hepatology Research

Hepatology Research 2014; 44: E240–E252 doi: 10.1111/hepr.12275

Original Article

Effect of the infectious dose and the presence of hepatitis C virus core gene on mouse intrahepatic CD8 T cells

Yutaka Horiuchi,[1] Akira Takagi,[1] Nobuharu Kobayashi,[1] Osamu Moriya,[1] Toshinori Nagai,[2] Kyoji Moriya,[3] Takeya Tsutsumi,[3] Kazuhiro Koike[3] and Toshitaka Akatsuka[1]

Departments of [1]Microbiology and [2]Pathology, Saitama Medical University, Saitama, and [3]Department of Gastroenterology, Graduate School of Medicine, The University of Tokyo, Tokyo, Japan

Aim: Chronic hepatitis C viral (HCV) infections often result in ineffective CD8 T-cell responses due to functional exhaustion of HCV-specific T cells. However, how persisting HCV impacts CD8 T-cell effector functions remains largely unknown. The aim of this study is to examine the effect of the infectious dose and the presence of HCV core gene.

Methods: We compared responses of intrahepatic CD8 T cells during infection of wild-type or HCV core transgenic (Tg) mice with various infectious doses of HCV-NS3-expressing recombinant adenovirus (Ad-HCV-NS3).

Results: Using major histocompatibility complex class I tetramer and intracellular interferon (IFN)-γ staining method to track HCV-NS3-specific CD8 T cells, we found that a significant expansion of HCV-NS3-specific CD8 T cells was restricted to a very narrow dosage range. IFN-γ production by intrahepatic CD8 T cells in HCV core Tg mice was suppressed as compared with wild-type mice. Higher levels of expression of regulatory molecules, Tim-3 and PD-1, by intrahepatic CD8 T cells and PD-L1 by intrahepatic antigen-presenting cells were observed in HCV core Tg mice following Ad-HCV-NS3 infection, and the expression increased dependent on infectious dose. Furthermore, we found a significant inverse correlation between the percentages of IFN-γ-producing cells and expression of regulatory molecules in antigen-specific intrahepatic CD8 T cells.

Conclusion: High infectious dose and the presence of HCV core gene were strongly involved in ineffective CD8 T-cell responses. We consider that HCV core Tg mouse infected with high infectious dose of Ad-HCV-NS3 is useful as a chronic infection model in the development of immunotherapy for chronic hepatitis C.

Key words: core, functional exhaustion, hepatitis C, infectious dose, T cell

INTRODUCTION

HEPATITIS C VIRUS (HCV) is a positive-sense single-stranded RNA virus of the genus *Hepacivirus* in the family *Flaviviridae*, and it infects 170 million people worldwide.[1] Approximately 10–60% of the patients clear HCV spontaneously during the acute phase of infection,[2] while the others develop chronic persistent HCV infection that eventually leads to liver cirrhosis and hepatocellular carcinoma.[3] HCV-specific cytotoxic T lymphocytes (CTL) play a major role in viral control during acute infection.[4] Nevertheless, during persistent infection, HCV-specific CTL effector functions are significantly impaired.

T-cell exhaustion is one of the remarkable features of chronic HCV infection. In chronically HCV-infected individuals, the frequencies of CTL are relatively low; similarly, the proliferative capacity as well as effector functions of HCV-specific T cells are impaired, and the production of type I cytokines (i.e. interleukin-2 and interferon [IFN]-γ) is dramatically suppressed.[5–8]

It appears that the major factors which determine duration and magnitude of an antiviral immune response are antigen (Ag) localization, dose and kinetics.[9] For example, high doses of widely disseminating strains of lymphocytic choriomeningitis virus (LCMV) exhaust antiviral CTL leading to establishment of a persistent infection.[10] Physical deletion of anti-LCMV CTL is most likely preceded by their functional impairment with the inability to produce effector cytokines.[11,12]

Correspondence: Professor Toshitaka Akatsuka, Department of Microbiology, Faculty of Medicine, Saitama Medical University, 38 Morohongo, Moroyama-cho, Iruma-gun, Saitama 350-0495, Japan. Email: akatsuka@saitama-med.ac.jp
Received 21 May 2013; revision 8 November 2013; accepted 11 November 2013.